ASTRONOMY & ASTROPHYSICS
SUPPLEMENT SERIES

Astron. Astrophys. Suppl. Ser. **42**, 251-281 (1980)

THE SPATIAL DISTRIBUTION OF THE INTERSTELLAR EXTINCTION

Th. NECKEL and G. KLARE

T. N., Max-Planck-Institut für Astronomie, D-6900 Heidelberg-Königstuhl, Federal Republic of Germany
G. K., Landessternwarte, D-6900 Heidelberg-Königstuhl, Federal Republic of Germany

Received December 12, 1979, accepted March 11, 1980

Summary. — Extinction values and distances have been computed from *UBV*, MK and β data for more than 11 000 O to F stars, including 7 565 O and B stars. For 1 020 stars two independent distance moduli were derived using M_v (MK) as well as M_v (β). The mean value of their differences is less than $0^m.01$.

With the aid of photographs of the Milky Way 325 fields in the galactic belt $| b | \leq 7°.6$ were demarcated in which the extinction and the star density is rather homogeneous. The $A_v(r)$ diagrams (Fig. 6) of these fields (Fig. 5) are discussed. From the fields with the most reliable A_v (r)-relations the galactic distribution of the dust up to 3 kpc (Fig. 8) has been derived.

Key words : Interstellar extinction — Galactic structure.

1. **Introduction.** — One of the main characteristics of the interstellar extinction A_v is its irregular structure. This makes it difficult to derive a detailed map of A_v as a function of position on the sphere and distance. Such a map offers the only direct possibility to derive the spatial distribution of the interstellar dust. Furthermore, for many investigations of galactic and extragalactic objects the value of A_v in the direction to the object under consideration is an important quantity. The easiest way to get detailed information on A_v as a function of the galactic coordinates l and b and the distance r is an analysis of color excesses and distances of individual stars. Several investigations of this kind have been published. Frequently used are those of Neckel (1967) and Fitzgerald (1968). Though these studies already use data for about 5 000 stars, numerous regions of the sphere still lack information on the extinction. It is still sometimes necessary to use the antiquated cosecant law for an estimation of the galactic extinction.

In the past ten years new data have become available so that the total number of stars for which extinction and distance values can be derived has increased to more than 11 000. This enables us to achieve a considerable improvement of the extinction analysis. In this paper we present results for low galactic latitudes, $| b | \leq 7°.6$. The data for the higher latitudes will be published in a subsequent paper.

2. **The *UBV*, MK and β data.** — For the determination of the distance to a star and the value of interstellar extinction in front of it we need the following quantities : (i) Apparent magnitude and color, for which we use photoelectrically measured *UBV*-data. (ii) Absolute magnitude and intrinsic color. These quantities can be derived in two independent ways : First from the MK spectral type by applying the MK-calibrations for absolute magnitudes and intrinsic colors and second from the Hβ index using the relation between M_v and β. In this case the intrinsic colors may be determined from the *UBV* data in combination with $M_v(\beta)$. Also the equivalent width of the Hγ line may be used as a measure of the luminosity. Hγ line measurements are available for about 1 200 stars (e.g. Crampton *et al.*, 1973). For 80 % of them the MK types and for 30 % the β indices are known. So the inclusion of the γ values would enlarge our material not considerably. Therefore we did not use them.

We have collected the existing, *UBV*, MK and β data for stars of type O, B and A as completely as possible. If stars of later spectral types are bright enough to have been observed, they are usually nearby and do not show an appreciable amount of extinction. Therefore we have not completely included F stars into our data collection. In addition we have adopted the distances and extinction values for Cepheids and galactic clusters compiled in the catalogue of extinction values by Neckel (1967). The photoelectric catalogues from Blanco *et al.* (1970) and Mermilliod (1976), which were obtained on magnetic tape from the Centre de Données Stellaires in Strasbourg were very useful for compiling the data.

Since this collection of data, especially the data for the O and B stars, should be valuable for other problems, we have included O and B stars even if the data necessary for the determination of extinction and distance was incomplete. It should also be clear which stars need further observations.

The coordinates of about 50 % of the collected stars

Send offprint requests to : Th. Neckel.

were taken from the Catalogue of Stellar Identification (CSI), or from the SAO catalogue. The coordinates of the remaining stars are from the sources listed in table I.

The origin of the MK types, the *UBV* data and the β values is tabulated in table I. The number of stars in 5° intervals of galactic longitude l as a function of l is shown in figure 1 for all stars as well as for those with galactic latitudes $| b | < 7.°6$. Figure 2 shows the frequency distribution of the V magnitudes. In column 1 of table II the numbers of stars for different spectral types are given. (For stars with no MK-types, spectral types were derived from photometric data.) The following columns give the number of stars with known MK spectral types, β indices and *UBV* data respectively.

Altogether our catalogue includes 11 072 objects, among them 7 565 O and B stars. In the near future the catalogue can be ordered from the Centre de Données Stellaires, in Strasbourg.

3. **Absolute magnitudes.** — For many studies dealing with galactic structure the absolute magnitudes M_v are the most problematic quantities. For a single early type star it is impossible to reach an accuracy better than about $0^m.5$. This is true, if M_v results either from the MK type or from the β index. Of course, the mean value of both methods has the best accuracy.

In order to avoid systematic deviations between the M_v resulting from both methods, we have used the M_v (MK) to calibrate the β index in terms of absolute magnitudes. The underlying calibration of MK types in terms of M_v is that of Schmidt-Kaler (1965). By means of 419 stars from the catalogue of 1 660 southern OB stars (Klare and Szeidl, 1966) without indications of emission, whose β-indices were measured by Klare and Neckel (1976) and whose MK types are known from the literature, we have derived a $M_v(\beta)$ calibration curve, which was already published in an earlier paper (Neckel and Klare, 1976). In the meantime the number of known MK types for the southern OB stars has been increased by new MK types for 1 090 objects by Garrison *et al.* (1977). We therefore could omit the less accurate MK types from the Michigan catalogue (Houk *et al.*, 1975), which were part of our data for our first calibration. For this reason we have repeated the $M_v(\beta)$ calibration.

After rejecting stars with possible emission in Hβ, with « *n* » characteristics or with uncertain MK types, 630 stars remained. Their M_v(MK) and β values were used for a least squares fit to the equation

$$M_v(\mathrm{MK}) = M_v(\beta) + kD_{U-B} . \qquad (1)$$

We approximate $M_v(\beta)$ by straight line segments through 10 points. D_{U-B} is the vertical distance of a star in the *U-B/B-V* two-color-diagram from the reddening path according to its MK type. (For more details see Neckel and Klare, 1976.) Errors in the spectral type cause a $D_{U-B} \neq 0$ which is correlated with the corresponding error in M_v. The term kD_{U-B} therefore partly corrects errors in the MK classification. From the least squares fit we find $k = -4.90 \pm 0.57$, very similar to the value from our earlier calibration (-5.03 ± 0.70). Figure 3 shows the solution for $M_v(\beta)$ together with the individual M_v(MK) corrected by the term $-kD_{U-B}$. The final calibration curve, which is tabulated in table III together with the data from our 1976-calibration, results from the smoothed straight line segments.

As we have shown, the correction term kD_{U-B} improves the absolute magnitudes derived from the MK types. Therefore we have applied this term to *all* M_v(MK), except for known as well as for suspected emission stars. Often they have an ultraviolet excess and therefore their D_{U-B} is not caused by a classification error. All stars with $D_{U-B} < -0.1$ are regarded as possible emission stars, because it is likely that such a high D_{U-B} is caused by emission rather than by a classification error.

Undoubtedly all existing MK calibrations are not free of errors which may reach some tenth of a magnitude. Especially the absolute magnitudes of the O type supergiants as well as those of B0-B2 main-sequence stars are certainly questionable (see for example FitzGerald *et al.*, 1979). The classification for the O and early B stars was improved by Conti and Alschuler (1971) and Walborn (1972) using finer spectral criteria. Some hundred stars were reclassified by them and a M_v(MK) calibration appropriate to their classification system was derived (Crampton and Georgelin, 1975). Because we have only MK types in the original system for the most O and early B stars in our material we decided to use throughout the original types in order to avoid inhomogeneities.

4. **Extinction values and distances.** — The visual extinction A_v can be derived from

$$A_v = R \{ (B - V) - (B - V)_0 \} . \qquad (2)$$

For R we take the value 3.1.

The intrinsic color $(B\text{-}V)_0$ follows directly from the MK calibration, if the MK type is known. In addition, $(B\text{-}V)_0$ can also be derived from the *UBV* and β data. The distance moduli are then given by

$$V - M_v - A_v = 5 \lg r - 5 . \qquad (3)$$

If we could derive A_v and r by both methods, we could use the mean values of extinction and distance moduli. This was possible for 1 020 stars. Figure 4 shows the frequency distribution of the differences

$$D = (V - M_v(\mathrm{MK}) - A_v(UBV, \mathrm{MK})) - \\ - (V - M_v(\beta) - A_v(UBV, \beta)) . \qquad (4)$$

Obviously, this is nearly symmetric to $D = 0^m.00$. If we exclude only the 38 stars with $| D | > 2^m.00$, we get a mean difference between the two independent distance moduli of 982 stars of $\bar{D} = -0^m.006$. This demonstrates impressively that there are no systematic differences between the distances derived from M_v(MK) and $M_v(\beta)$.

The rms of D amounts to $0^m.65$. If Δ_{MK} and Δ_β are the mean errors of the two distance moduli, we get

$$0^m.65 = \sqrt{\Delta_{MK}^2 + \Delta_\beta^2} . \qquad (5)$$

To this number contribute : i) The cosmic scatter in the M_v(MK) relation and the uncertainties of the MK types, which cause an error $\Delta M_v(\mathrm{MK}) = \Delta_{MK}$. For ΔM_v(MK) usually $0^m.50$ is assumed. ii) The cosmic scatter in the

$M_v(\beta)$ relation and the errors of the β measurements (which amount in the mean to about $0^m.008$ resulting to an error of M_v $(\beta) \sim 0^m.30$, see table III). From equation (5) it follows with $\Delta M_v(\mathrm{MK}) = 0^m.50$ a total error $\Delta M_v(\beta) = 0^m.42$ indicating only a small contribution of the cosmic scatter of the $M_v(\beta)$ relation to the observed scatter $0^m.65$. Of course, the small difference between $\Delta M_v(\mathrm{MK})$ and $\Delta M_v(\beta)$ is not significant.

Assuming $\Delta_{\mathrm{MK}} = \Delta_\beta = \Delta$, we find $\Delta = 0^m.46$. Finally the error of the mean value of the two distance moduli,

$$\overline{(m - M)} = 0.5 \{ [V - M_v(\mathrm{MK}) - A_v(UBV, \mathrm{MK})] + [V - M_v(\beta) - A_v(UBV, \beta)] \}$$

turns out to be

$$\frac{1}{2}\sqrt{2}\,\Delta = 0^m.33 .$$

The error in the distances is roughly 25 %, if only one determination of M_v is available, and 16 %, if both M_v are known. Compared to this relatively large error the uncertainties of the derived A_v are negligible. We expect them to be in the range from $0^m.1$ to $0^m.2$.

6. **The method of the extinction analysis.** — A dust cloud is recognizable by the fact that the extinction A_v is higher behind the cloud than in front of it. So the most natural method of analysing extinction data is to look for the variation of A_v with increasing distance in distinct areas of the sky. In doing this it must be taken into account that our data become increasingly incomplete with increasing extinction because stars with higher A_v values are usually faint and therefore poorly observed. In a field with a strong variation of extinction at a distinct distance, those parts with the highest obscuration are usually the least observed. This selection effect produces systematically too small A_v mean values. The error due to this selection effect is negligible only in fields with a small scatter of the A_v values. Quantitatively this is shown by Neckel (1966). From these considerations follows the necessity to use small fields with a scatter of A_v as low as possible.

Photographs of the Milky Way demonstrate the extremely inhomogeneous distribution of the dark matter in some regions. Often, the extinction varies rapidly within a few minutes of arc. In order to derive $A_v(r)$ up to distances of a few kpc in all areas of the Milky Way with sizes of some minutes of arc, data for many more stars than we have collected would be necessary. For this reason we used photographs of the Milky Way for additional information on extinction (for the northern sky, the POSS, and for the southern sky, the Würzburg atlas of the Southern Milky Way, Haffner *et al.*, 1969). We expect that in areas of uniform star density the extinction is also more or less homogeneously distributed up to some kpc distance. In such cases the A_v and r of a limited number of stars are regarded as samples representative of the mean $A_v(r)$ in the whole field considered. To enable a suitable comparison of the star data and the photographs, all stars in the galactic belt $| b | < 7°.6$ have been mapped and for each star A_v and r (in kpc) are noted. A galactic as well as an equatorial grid is overlayed on this map, a small part of which is shown in figure 7.

In the galactic belt $| b | < 7°.6$ we have chosen 325 fields in which to investigate the relationship between A_v and r. The boundaries of these fields are chosen such that within each field the star density is uniform to some extent and the extinction values show no significant variation over the field. This requirement often causes irregular boundaries of the fields. The most striking advantage of this method is the small resulting scatter in the $A_v(r)$ diagrams of most fields, so avoiding largely the influence of the selection effect.

If the number of stars with known A_v and r are too small or if the dust distribution is too chaotic, it is impossible to find fields small enough to represent the real behaviour of the extinction. In such a case the scatter in the $A_v(r)$ diagram is high an it can serve only as a rough information.

Figure 5 shows the map of our fields and figure 6 a to o, their $A_v(r)$ diagrams. Each field is designated by a running number as well as by the galactic coordinates l/b of a point near its center. Some parts of the galactic belt $| b | < 7°.6$ are not covered because of insufficient data. These are sometimes the regions with the highest dust concentrations in the Milky Way.

In deriving mean A_v values for each field, we did not approximate $A_v(r)$ by analytical functions to derive its parameters by a least squares fit because the irregular behaviour of the extinction cannot be described by a simple analytical function in most cases.

For example, we consider the $A_v(r)$ diagram of field 1. A map of this field is given in figure 7. Obviously A_v increases from 0 to about 1 kpc and remains constant at least up to 4 kpc. The scatter in the first kpc is mainly caused by errors in the absolute magnitudes respectively in the distance moduli. For the construction of $A_v(r)$ we use mean values A_v and r (r was computed from the mean values of the distance moduli) for groups of stars suitably chosen, in the case of field 1 for the stars within the A_v intervals $0^m.00 \ldots 0^m.40$, $0^m.40 \ldots 1^m.00$, $1^m.00 \ldots 1^m.50$. The stars with $A_v > 1^m.50$ and $r < 4$ kpc do not show any variation of A_v with distance. Therefore, $A_v(r)$ is equal to $\overline{A_v}$ for the stars in the range between the upper limit of the extinction rise and 4 kpc. In field 1 it is difficult to locate the limit of the extinction rise. However, the $A_v(r)$ diagrams of neighbouring fields 4, 9, 13, 14, 15, 18, 19 convincingly show that A_v increases only within $0 < r \leq 1$ kpc in this region of the sky. The same should be true also for field 1. Conclusions of this kind were drawn in many cases in constructing $A_v(r)$. The A_v (r) are shown as solid lines in figure 6 if the information only comes from data within the field considered and by dashed lines if information from neighbouring fields was used or if we did not have enough data for reliable mean values.

A strange feature of the $A_v(r)$ diagram for field 1 is worth mentioning : there are 3 stars at $r > 4$ kpc but with A_v values smaller than those in the interval 1 kpc $< r <$ 4 kpc. It seems unlikely that only the most distant stars are located in directions with unusually low

A_v. Figure 7 shows these 3 stars are not located near each other, which would indicate a part of this field has systematically lower extinction. Most probably this reflects errors of the MK types of these stars. Two of them are classified as Ib supergiants and the third as a luminosity class II giant. If they are in reality main-sequence stars, their A_v would be up to $0^m.25$ higher and their distances appreciably smaller. These changes would bring the 3 stars in among the others.

Sometimes single stars have A_v values much higher than all other nearby stars. Mostly these stars are exciting stars of HII regions with internal dust. Such cases are marked with the name of the associated HII region.

6. **The galactic distribution of the dust.** — Figure 8 shows the extinction up to a distance of 1 kpc. If the A_v (1 kpc) for neighbouring fields are within the same A_v-interval of figure 8, they are not recognizable as single fields. Several dark clouds are outlined in figure 8, for example at $l = 302°$ the well known coal sack. Between $l = 210°$ and $l = 250°$ the extinction is at lowest, whereas we find the highest A_v at galactic longitudes 350°...0°...150°.

From the most reliable $A_v(r)$ relations, the map of the galactic dust distribution up to 3 kpc, shown in figure 9a, has been constructed. It shows big complexes of dust extending up to 1 kpc. The areas between them are often nearly dust free. In the following we refer to the designations given in figure 9b. In table IVa the numbers of those fields are listed, whose $A_v(r)$ contribute to the localization of the dust complexes.

In contrast to the farther dust complexes the distances and details of those with $r \leq 1$ kpc should be reliable to a high degree, because data from many fields contributed to their construction. The fact that the regions between them are essentially really free of dust is illustrated by many $A_v(r)$ diagrams (see table IVb). At distances $r > 1$ kpc we have probably not detected all existing clouds. The lowest level in figure 9a ($a_v < 1^m.0$/kpc) was chosen at position, *l, r,* if there is at least one field at the galactic longitude l with $a_v < 1^m.0$/kpc at the distance r and no other field with a higher a_v. This does not exclude the possibility that additional data could reveal other complexes of dust for fields at the same l but with different latitudes b where we do not have enough information at present.

A striking feature of figure 9a is the fact that for $r < 1$ kpc the clouds are larger than for $r > 1$ kpc. This is most probably caused by the higher density of information at smaller distances. The dust complexes H, I, J, N, O, P, Q, R are quite likely connected with each other and form in reality one or two larger complexes as do A and B in the solar neighbourhood.

Comparing figures 8 and 9 with the corresponding figures of Neckel (1966), we see that because of the wider data base used in this work new features at greater distances have appeared and nearby features are better resolved.

In regions of star formation very high extinction values, up to $> 10^m$, are commonly observed. An example is the strong concentration of dust at $l = 80°$, associated with the Cyg OB II association. Here we find dust concentrations in the range $6...11^m$/kpc. Cloud H in figure 8 is probably part of the dust and molecular cloud associated with the HII region M17. Cloud H can be detected in the fields 241(11/ − 1), 245(13/ − 3) and 252(18/0), which are near to field 246(16/ − 1) in which M17 itself is situated. Usually, however, the apparent magnitudes of such highly obscured stars are too faint to be included in our work. Therefore the dense clouds associated with the most prominent regions of star formation can only occasionally be recognized in our data. For this reason it is not surprising that the dust clouds shown in figure 8 do not exhibit a clear correlation with the known spiral features in the solar neighbourhood.

Acknowledgements. — It is a pleasure to thank Prof. Dr. H. Elsässer for his interest and permanent promotion in this study. We are grateful to Prof. Dr. H. Scheffler and Dr. S. Kleiner for carefully reading the manuscript. We would like to thank Mrs. K. Dorn, Mrs. D. Gayer and Mr. W. Neumann for producing the numerous figures.

References

BEER, A. : 1961, *Mon. Not. R. Astron. Soc.* **123,** 191.
BIGAY, J. H., GARNIER, R., GEORGELIN, Y. P. and Y. M. : 1972, *Astron. Astrophys.* **18,** 301.
BLANCO, V. M., DEMERS, S., DOUGLASS, G. G., FITZGERALD, M. P. : 1970, *Publ. U. S. Nav. Obs.,* 2nd Series, **21.**
BUSCOMBE, W. : 1977, MK Spectral Classifications, 3rd General Catalogue (Evanston).
CONTI, P. S., ALSCHULER, W. R. : 1971, *Astrophys. J.* **170,** 325.
COUSINS, A. W. J., STOY, R. H. : 1963, *R. Obs. Bull.* **64.**
CRAMPTON, D. : 1971, *Astron. J.* **76,** 260.
CRAMPTON, D., LEIR, A., YOUNGER, F. : 1973, *Publ. Dom. Astrophys. Obs. Victoria* B.C. **XIV,** 8.
CRAMPTON, D., GEORGELIN, Y. M. : 1975, *Astron. Astrophys.* **40,** 317.
DEUTSCHMAN, W. A., DAVIS, R. J., SCHILD, R. E. : 1976, *Astrophys. J. Suppl. Ser.* **30,** 97.
FEAST, M. W., STOY, R. H., THACKERAY, A. D., WESSELINK, A. J. : 1960, *Mon. Not. R. Astron. Soc.* **122,** 239.
FITZGERALD, M. P. : 1968, *Astron. J.* **73,** 983.
FITZGERALD, M. P., LUIKEN, M., MAITZEN, H. M., MOFFAT, A. F. J. : 1979, *Astron. Astrophys. Suppl. Ser.* **37,** 345.
GARRISON, R. F., HILTNER, W. A., SCHILD, R. E. : 1977, *Astrophys. J. Suppl. Ser.* **35,** 111.
GEORGELIN, Y. M., GEORGELIN, Y. P., ROUX, S. : 1973, *Astron. Astrophys.* **25,** 337.
GOY, G. : 1973, *Astron. Astrophys. Suppl. Ser.* **12,** 277.
HAFFNER, H., NOWAK, T. : 1969, Würzburg Atlas Southern Milky Way.
HAVLEN, R. J. : 1978, *Astron. Astrophys.* **64,** 295.
HILL, P. W., LYNAS-GRAY, A. E. : 1977, *Mon. Not. R. Astron. Soc.* **180,** 691.
HILTNER, W. A., JOHNSON, H. L. : 1956, *Astrophys. J.* **124,** 367.
HOFFLEIT, D. : 1956, *Astrophys. J.* **124,** 61.
HOUCK, N., COWLEY, A. P. : 1975, University of Michigan, *Catalogue of Two-Dimensional Spectral Types for the HD Stars* **1.**
JOHNSON, H. L., BORGMANN, J. : 1963, *Bull. Astron. Inst. Neth.* **17,** 115.
KLARE, G., SZEIDL, B. : 1966, *Veröffentl. Landessternwarte Heidelberg-Königstuhl* **18.**
KLARE, G., NECKEL, Th. : 1977, *Astron. Astrophys. Suppl. Ser.* **27,** 215.
MERMILLIOD, J. Cl. : 1976, *Astron. Astrophys. Suppl. Ser.* **24,** 159 and CDS Strasbourg.
MORGAN, W. W., CODE, A. D., WHITFORD, A. E. : 1955, *Astrophys. J. Suppl. Ser.* **2,** 41.
NECKEL, Th. : 1966, *Z. Astrophys.* **63,** 221.
NECKEL, Th. : 1967, *Veröffentl. Landessternwarte Heidelberg-Königstuhl* **19.**
NECKEL, Th., KLARE, G. : 1976, *Astron. Astrophys.* **52,** 77.
NECKEL, Th. : 1979, unpublished *UBV,* data.
SCHMIDT-KALER, Th. : 1965, in H. H. Voigt (ed.), *Astronomie und Astrophysik* (Landolt-Börnstein, Springer Verlag Berlin-Heidelberg-New York).
SMITH, E., VAN P. : 1956, *Astrophys. J.* **124,** 43.
STROM S. E., GRASDALEN, G. L., STROM, K. M. : 1974, *Astrophys. J.* **191,** 111.
WALBORN, N. R. : 1973, *Astron. J.* **77,** 312.
WHITEOAK, J. B. : 1962, *Mon. Not. R. Astron. Soc.* **125,** 105.

TABLE I. — *References for MK, UBV and β data.*

Reference	MK	UBV	β
Blanco et al. (1970)	5501	6142	
Feast et al. (1960)	17	17	
Hoffleit (1956)	14	14	
Cousins et al. (1963)	3	4	
Bigay et al. (1972)	22	20	
Crampton (1971)	27	22	
Georgelin et al. (1973)	29	31	
Mermilliod (1976)	697	797	
Deutschman et al. (1976)	344	1612	1538
Goy (1973)	49	13	
Beer (1961)	10	11	
Whiteoak (1962)	11	10	
Johnson et al. (1963)	1	1	
Hill et al. (1977)	75	80	
Garrison et al. (1977)	1090		
Havlen (1978)		10	10
Neckel (1967)	238		
Strom et al. (1975)	33	33	
Hiltner et al. (1956)	1	1	
Smith (1956)	1	1	
Morgan et al. (1955)	22	26	
Buscombe (1977)	8	8	
Klare et al. (1977)		1659	1659
Neckel (1979)		86	82

TABLE III. — *The new $M_V(\beta)$ calibration compared with our previous calibration (1976).*

β	$M_V(\beta)$ (new)	$M_V(\beta)$ (1976)
2.53	-7.03	-7.30
2.54	-6.52	-6.72
2.55	-6.05	-6.28
2.56	-5.70	-5.92
2.57	-5.42	-5.56
2.58	-5.18	-5.22
2.59	-4.95	-5.00
2.60	-4.66	-4.65
2.61	-4.12	-4.25
2.62	-3.61	-3.75
2.63	-3.20	-3.22
2.64	-2.80	-2.77
2.65	-2.47	-2.45
2.66	-2.23	-2.23
2.67	-2.08	-2.08
2.68	-1.9	-1.9
2.69	-1.7	-1.7

TABLE II. — *Total numbers of stars in different spectral type intervals and numbers of stars with known MK-types, β-indices and UBV data.*

Type	Total	MK	β	UBV
O	767	617	242	730
BO...B1	1800	1460	670	1761
B1.5...B3	2219	1576	851	2172
B3.5...B6.5	1172	634	553	1141
B7...B9.5	1607	1090	663	1475
A	1666	1666	66	1451
F	1224	1224	6	1189
gal. Clusters	129			
δ Cep-stars	204			

TABLE IVa. — *Numbers of fields which contribute to the localization of dust clouds A...X (Fig. 9).*

A	35 139 147 150 155 176 209 210 211 245 260 266 272 279 284 290 291 295
B	1 4 14 15 18 20 23 24 25 27 28 29 33 40 47 48
C	51 52 53 60
D	65 68 71 76
E	86 89 91 98
F	94 99 100 103 105 107 108 110 111 113 118
G	136 159 160 167 173 176 179 180 181 184 187 190 192 193 194 201 202 203 204 205 209 210 211 215 222 223 224 231
H	241 245 252
I	209 215
J	178
K	157
L	123 124 126 127
M	144
N	173 175
O	166
P	157
Q	148
R	133
S	99
T	68 69
U	40 42
V	25 26
W	310 313 314
X	273

TABLE IVb. — *Numbers of fields, whose $A_V(r)$-diagrams show regions nearly free of dust.*

Region between A and B:	285,286, 288, 289, 290, 291, 293, 295
Region in front of D:	86, 88, 89, 91, 94
Region in front of F:	98, 99, 104, 107, 108, 109, 110, 111, 113, 118

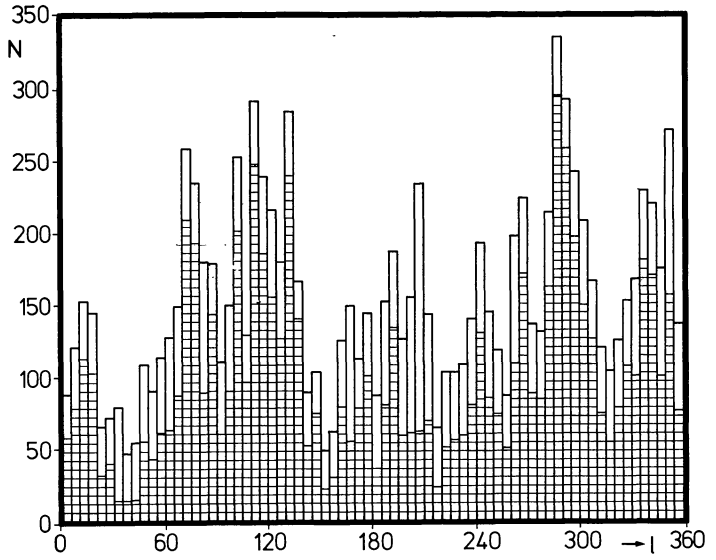

FIGURE 1. — Distribution of the stars *versus* galactic longitude. Hatched : stars with $| b | < 7°6$.

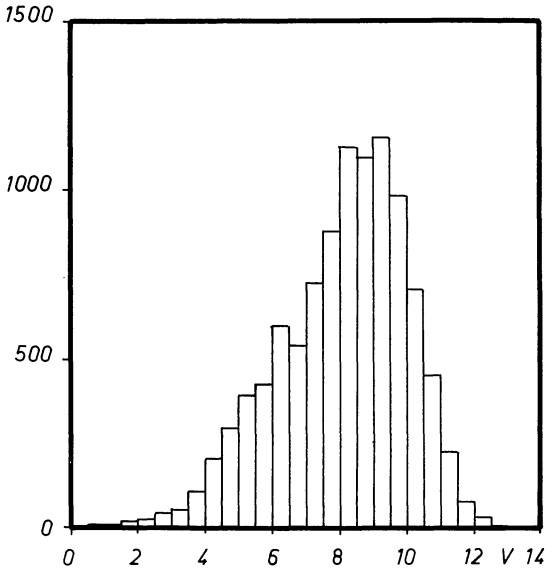

FIGURE 2. — Distribution of the stars *versus* apparent *V*-magnitude.

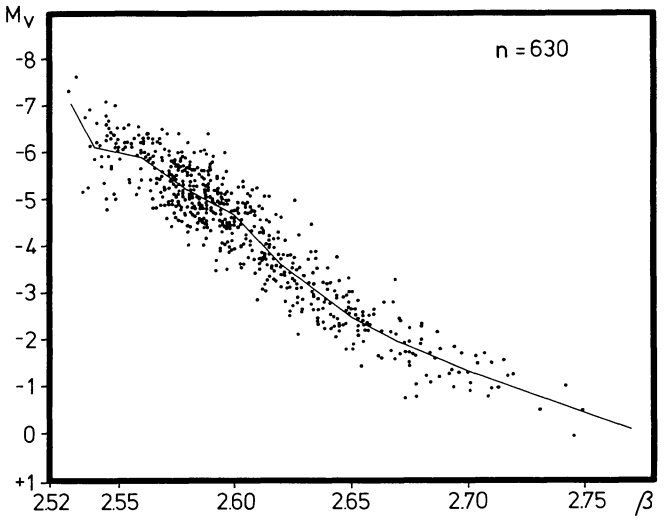

FIGURE 3. — Corrected absolute magnitude M_v according to equation (1) *versus* β.

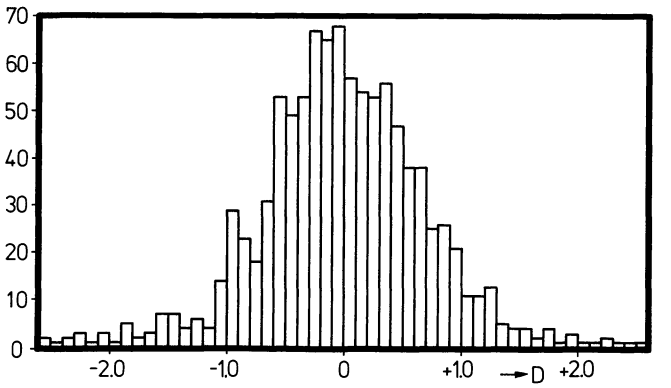

FIGURE 4. — Frequency distribution of the differences between the distance moduli derived from *UBV* + MK and *UBV* + β data.

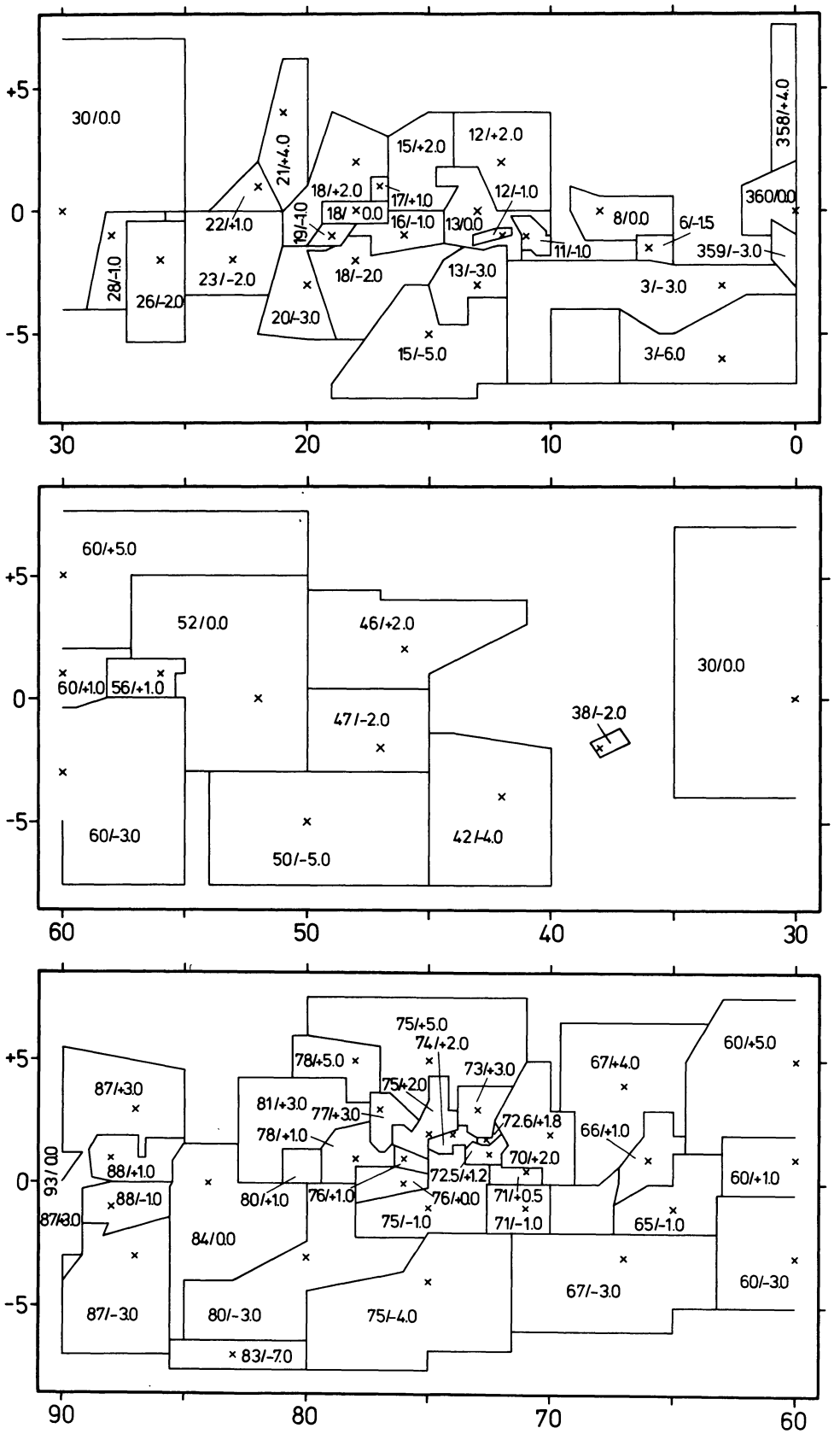

FIGURE 5a.

FIGURE 5. — Map of the 325 fields, whose $A_v(r)$-diagrams are shown in figure 6.

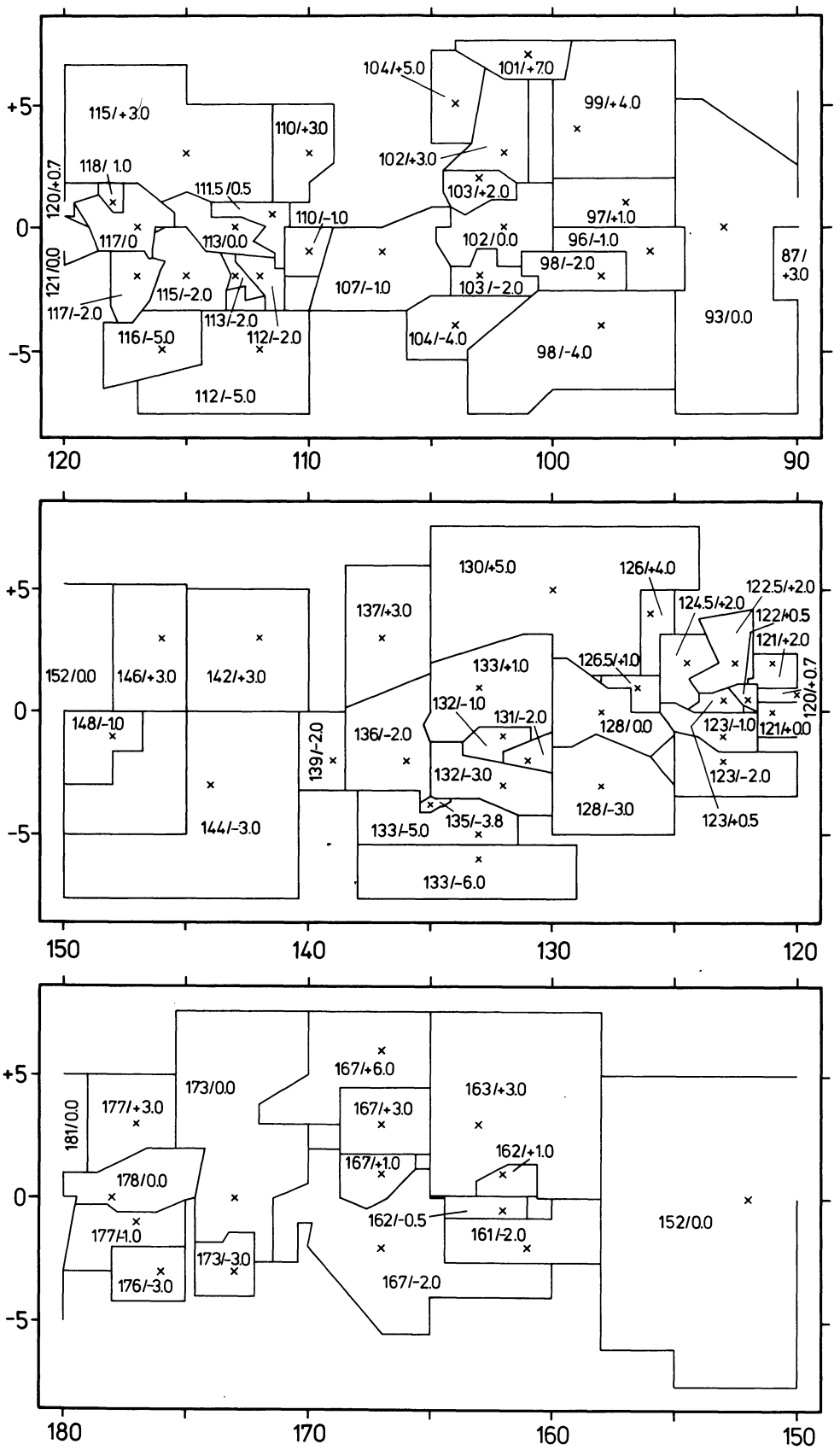

FIGURE 5b.

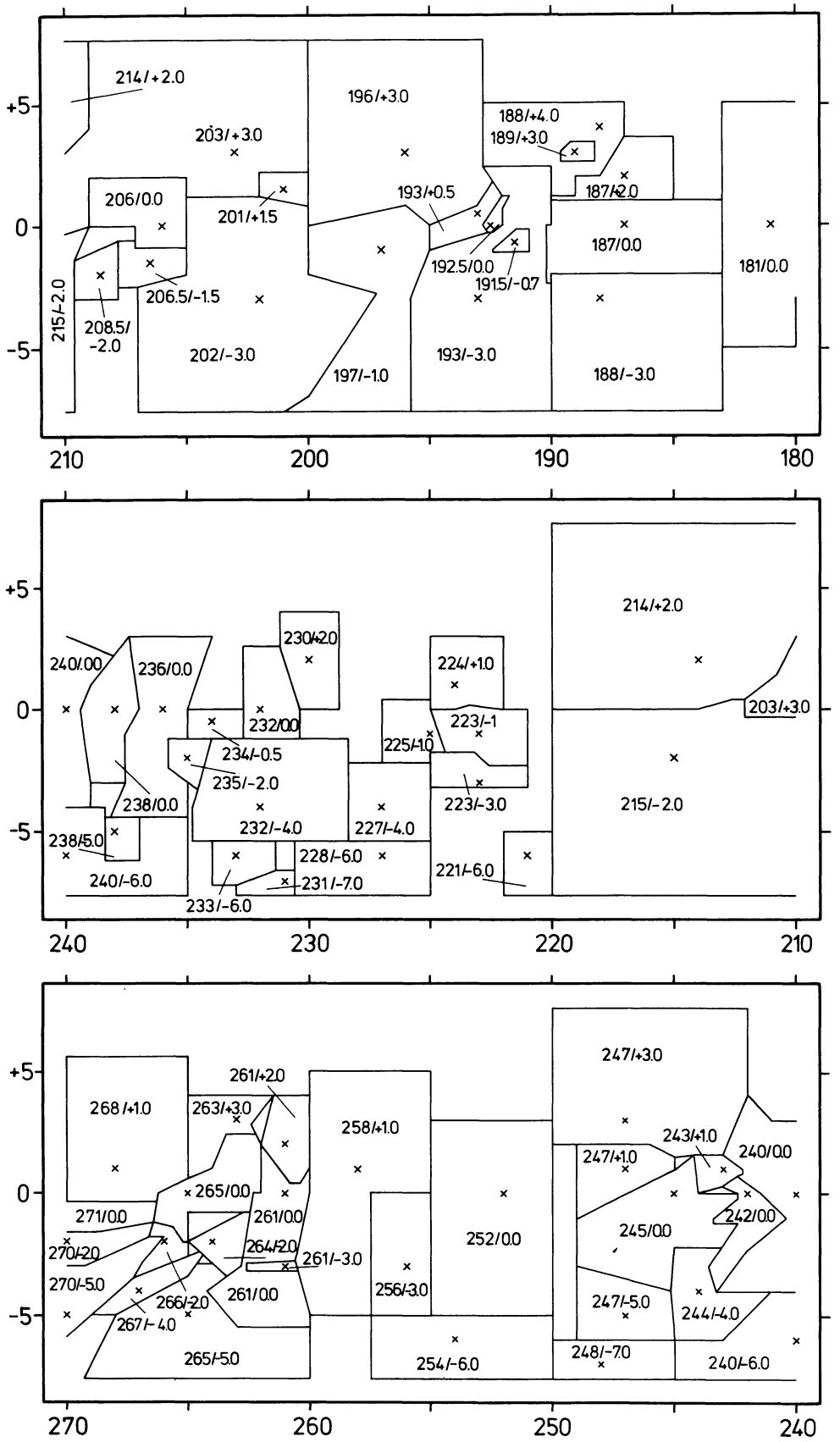

FIGURE 5c.

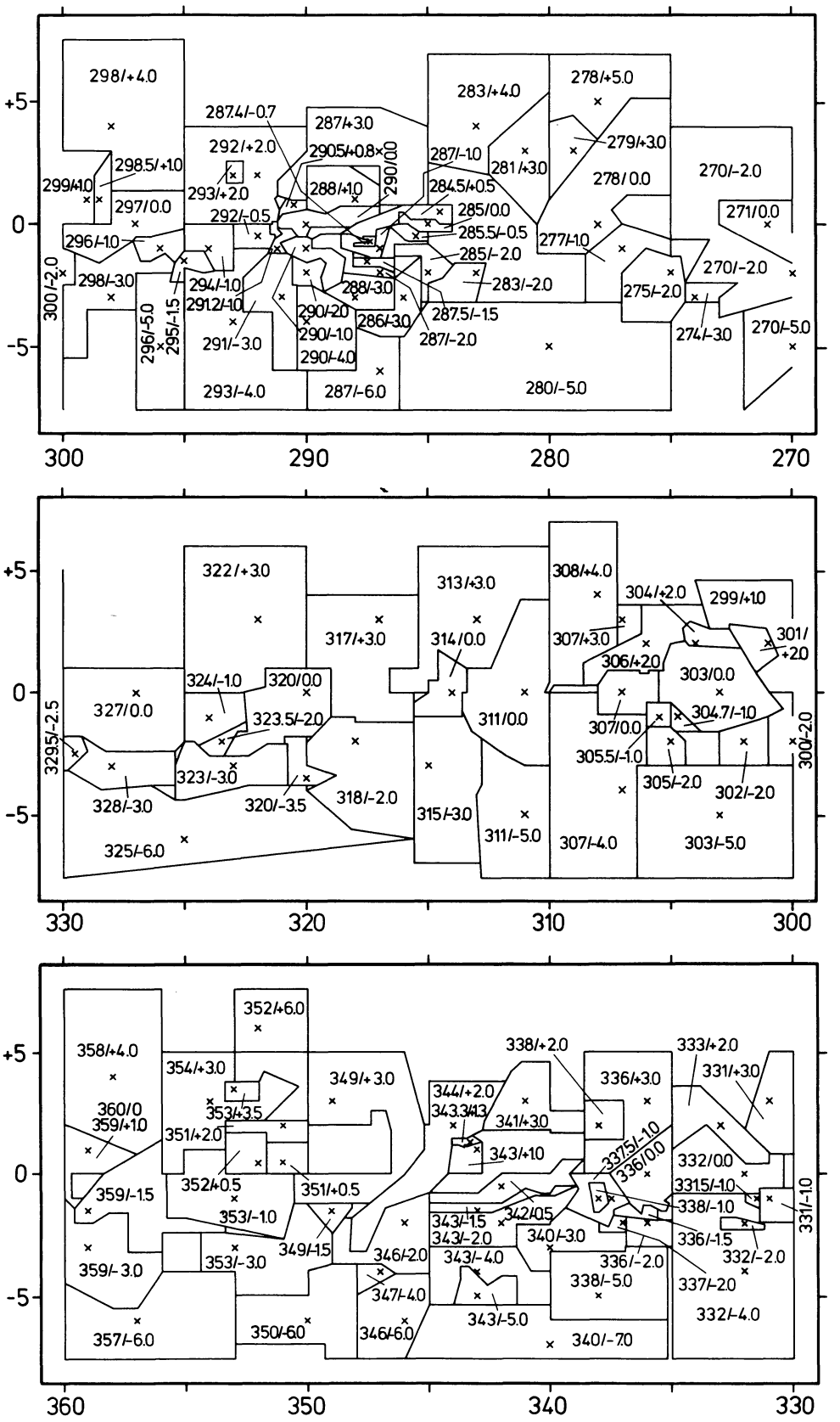

FIGURE 5d.

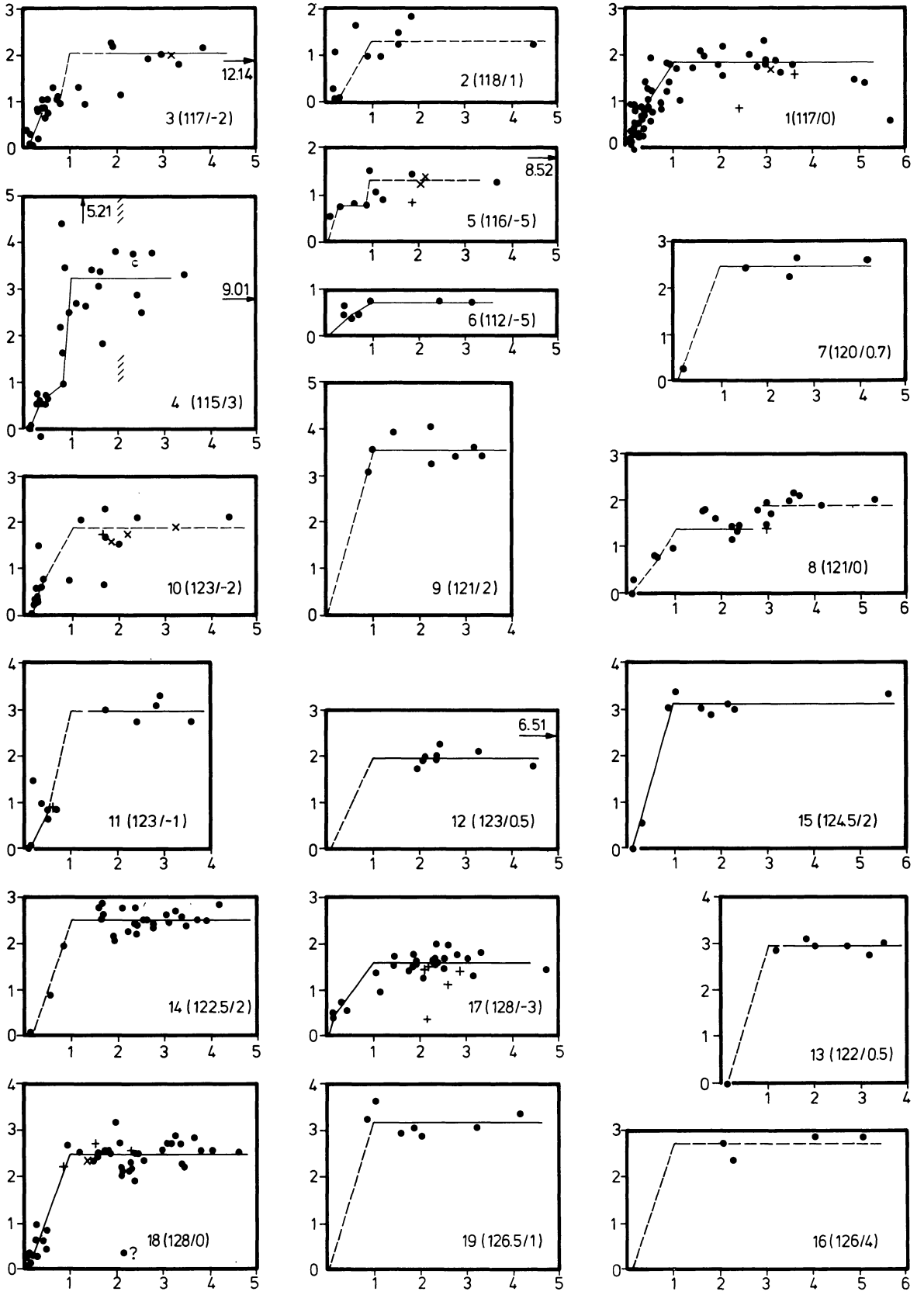

FIGURE 6a.

FIGURE 6. — $A_v(r)$-diagrams of the 325 fields shown in figure 5.

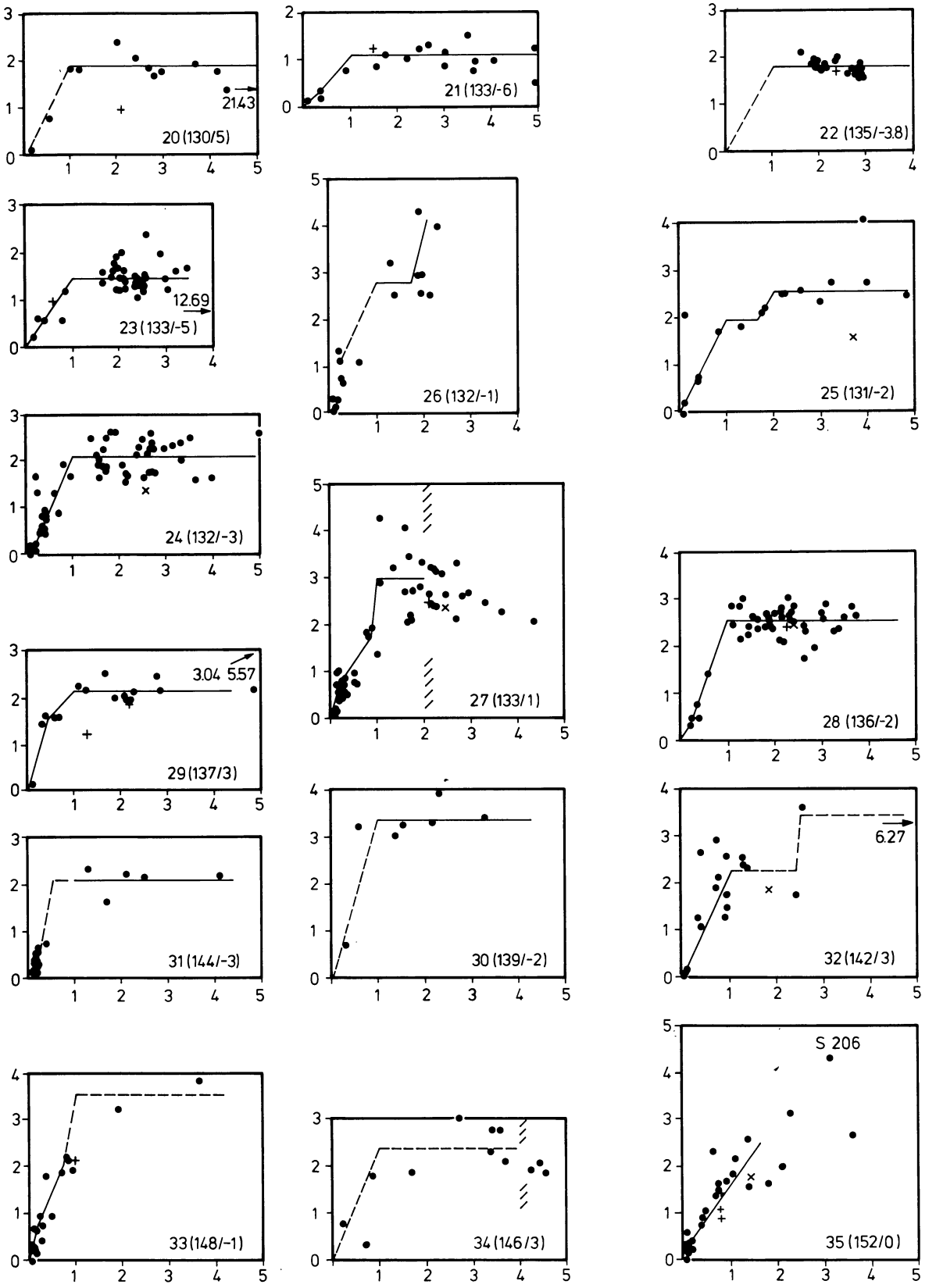

FIGURE 6b.

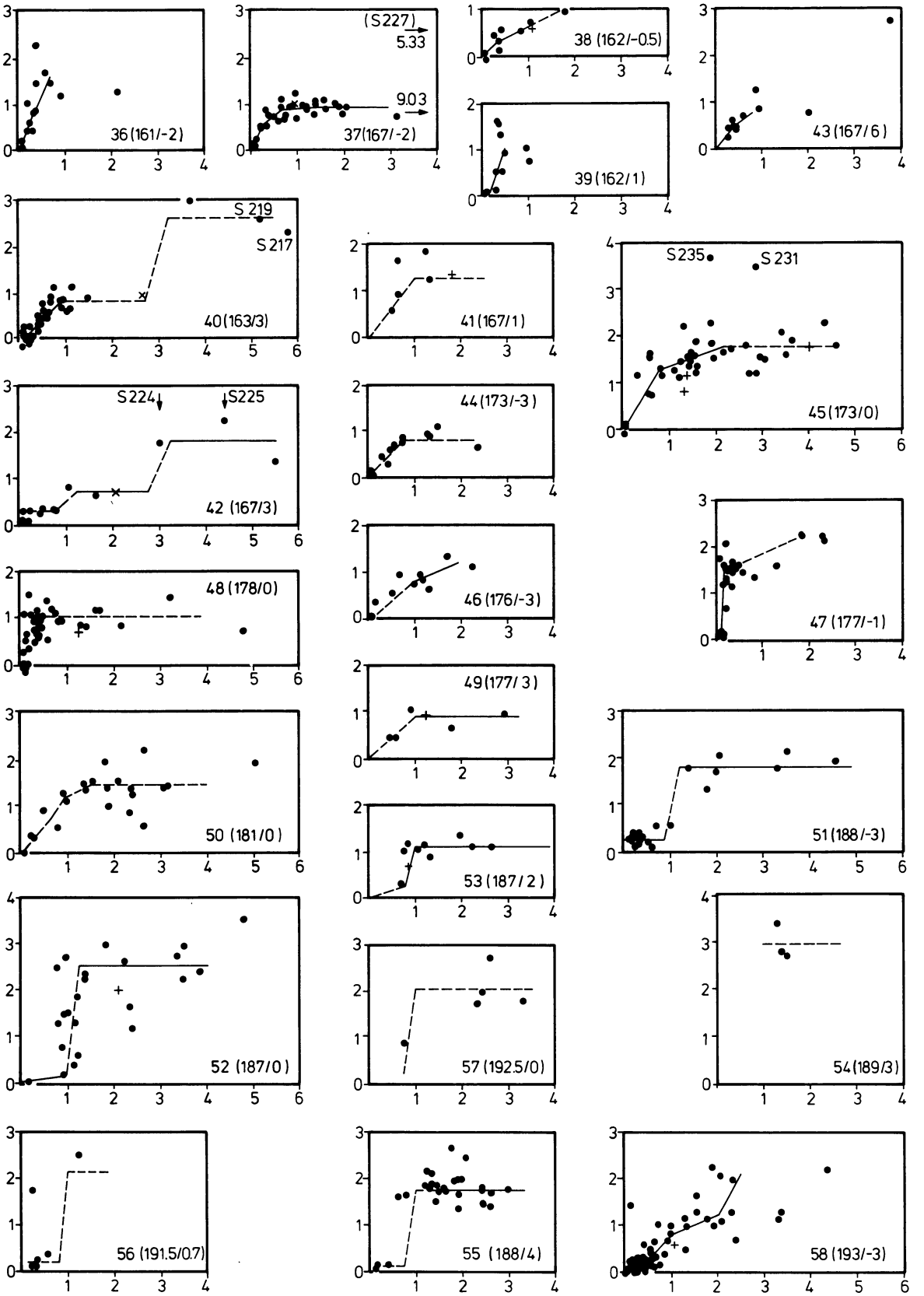

FIGURE 6c.

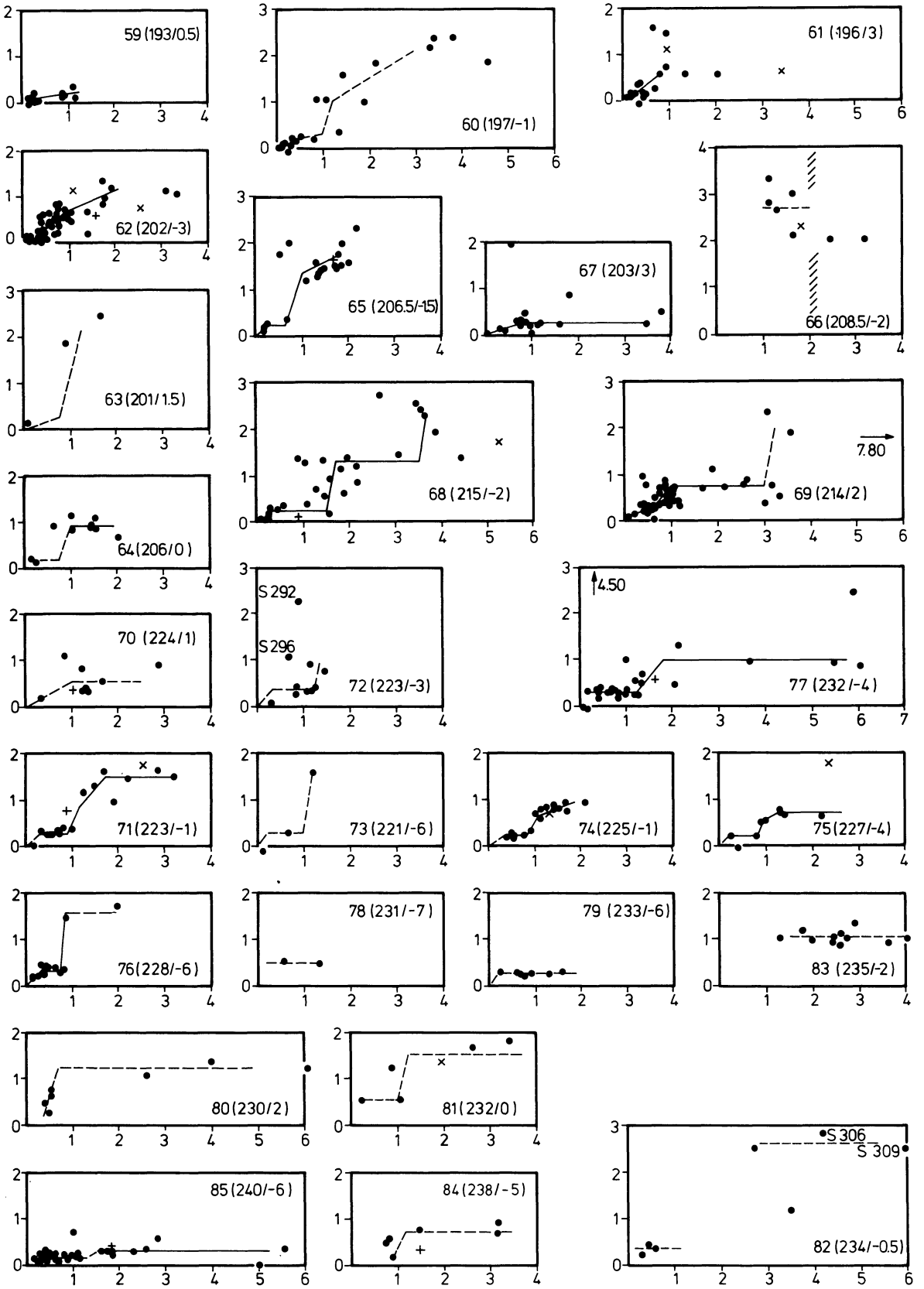

FIGURE 6d.

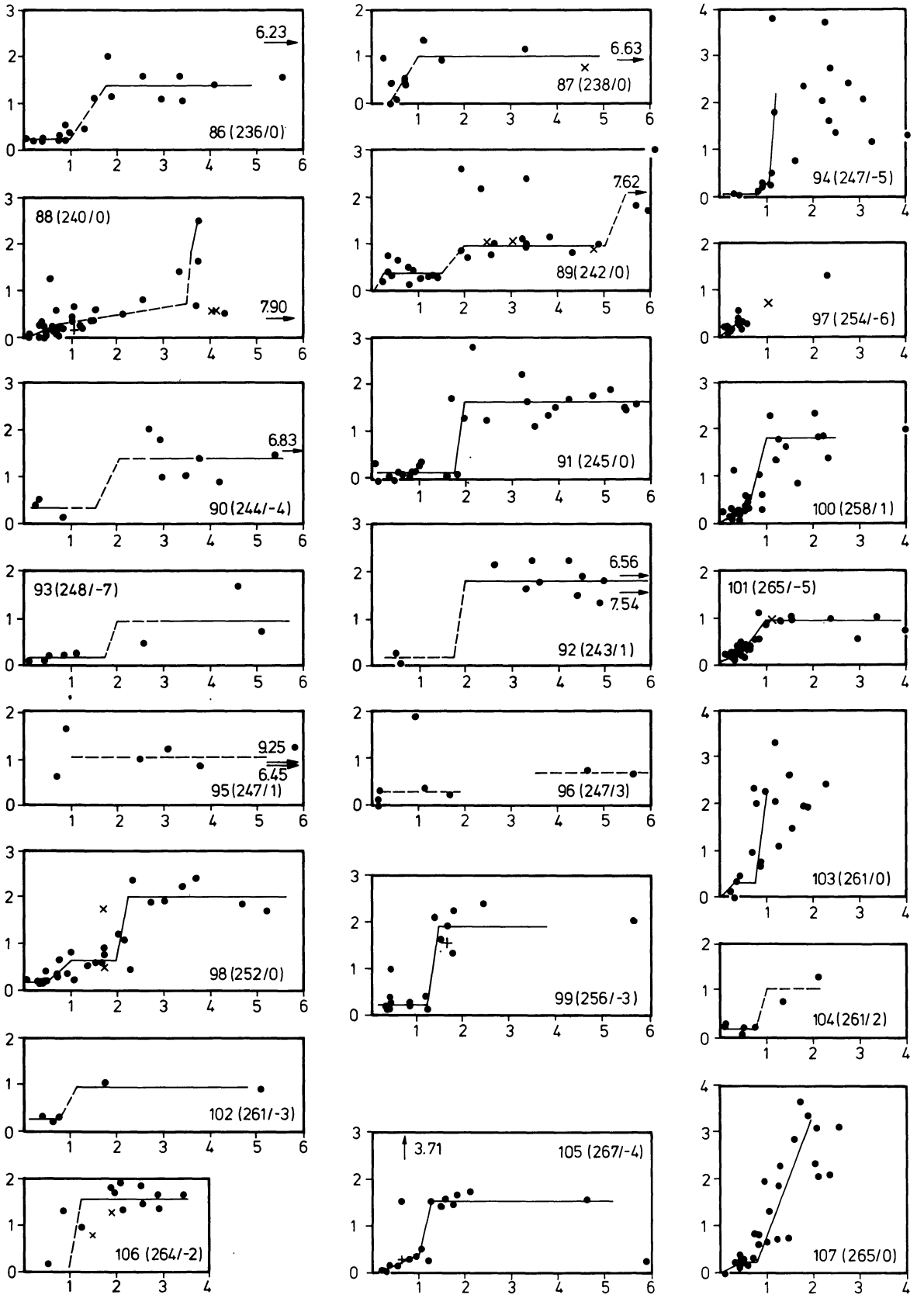

FIGURE 6e.

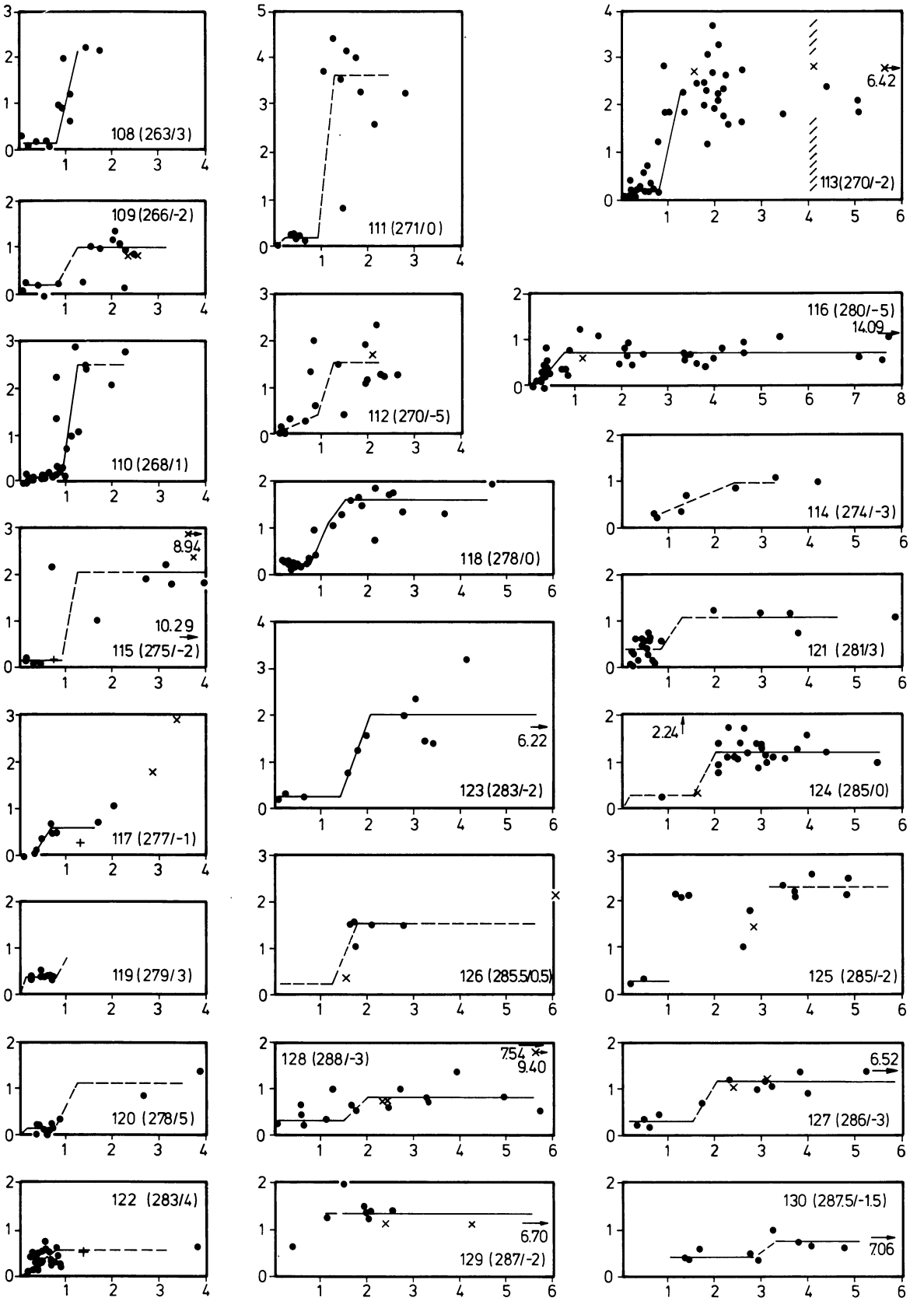

FIGURE 6f.

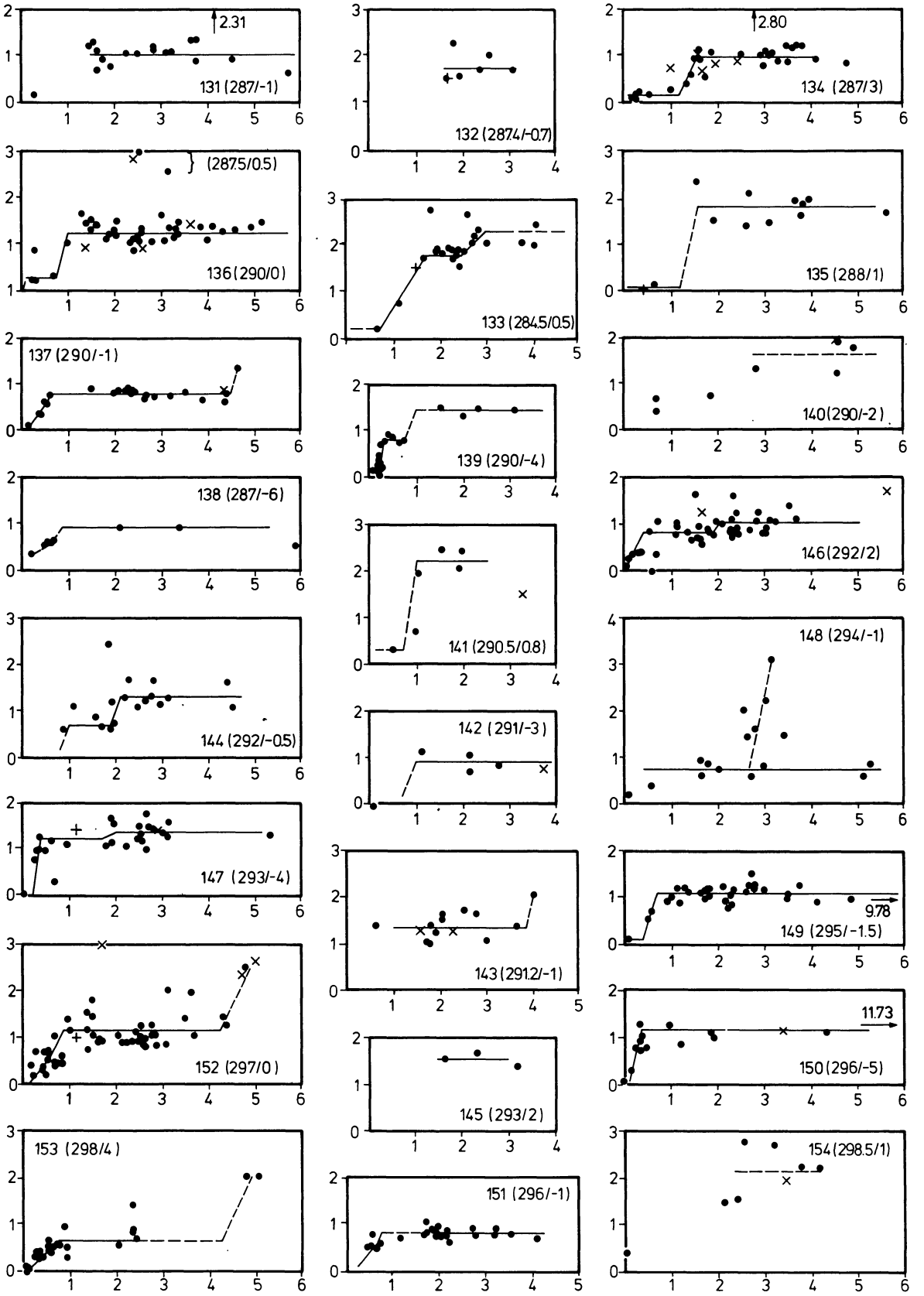

FIGURE 6g.

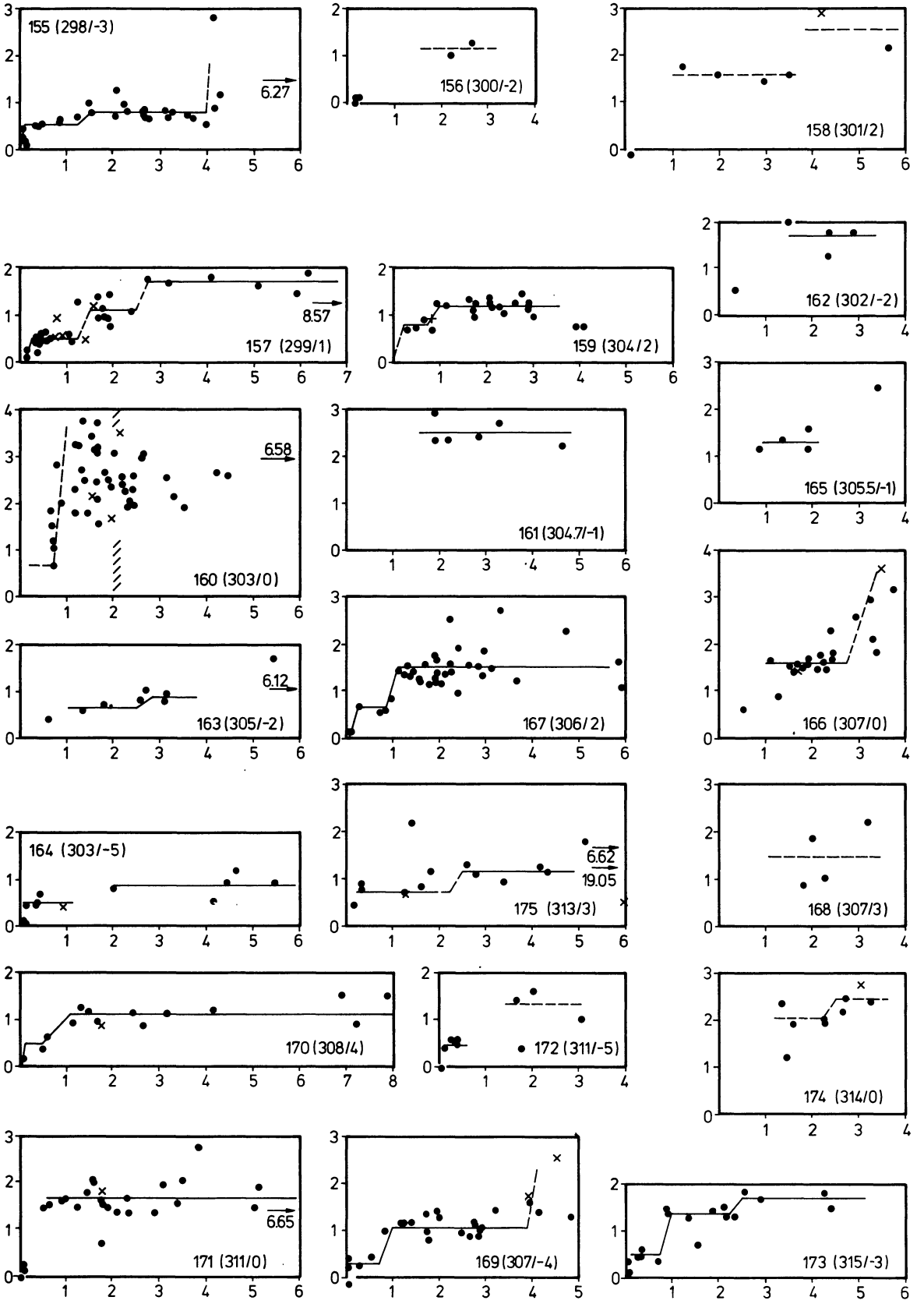

FIGURE 6h.

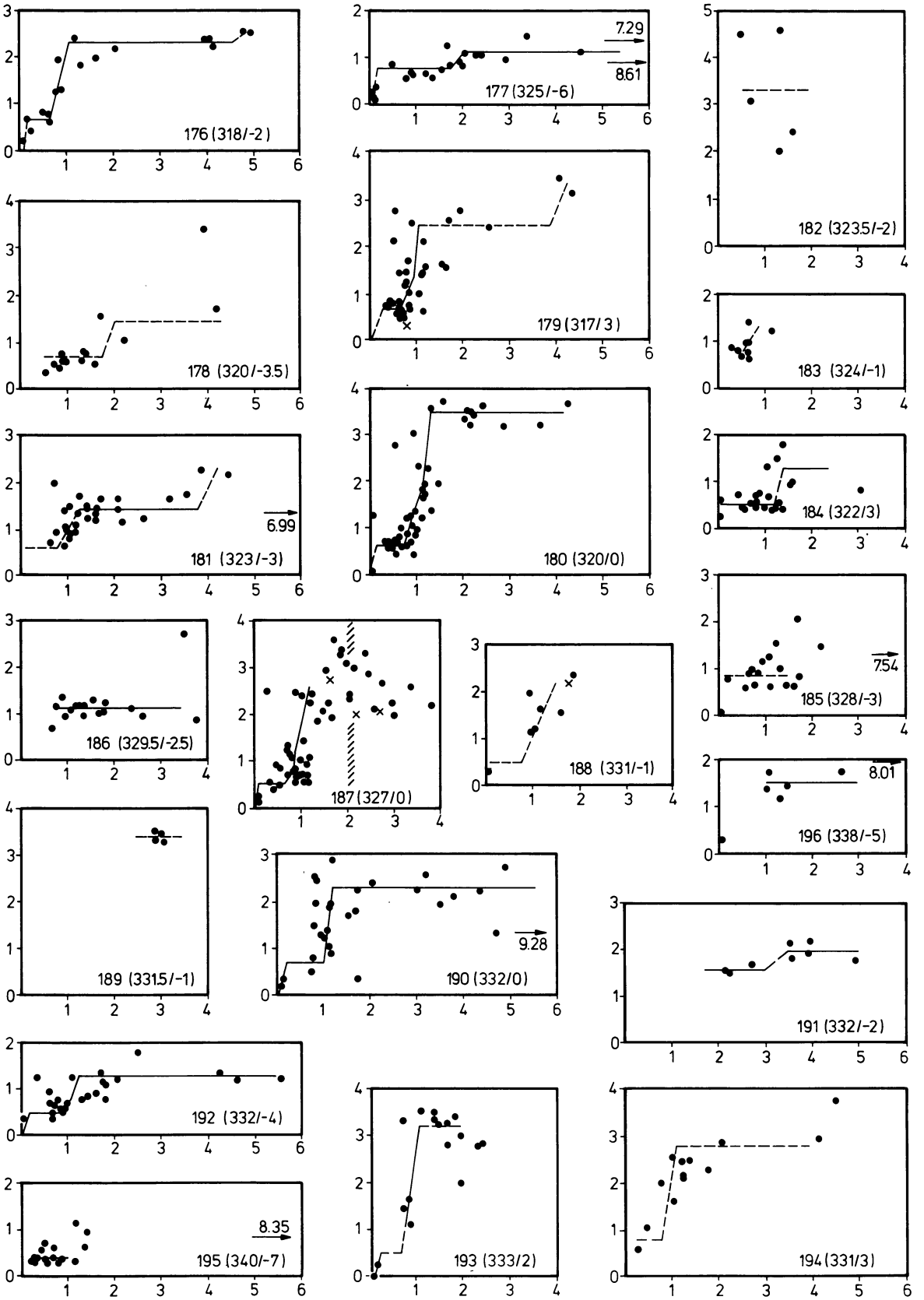

FIGURE 6i.

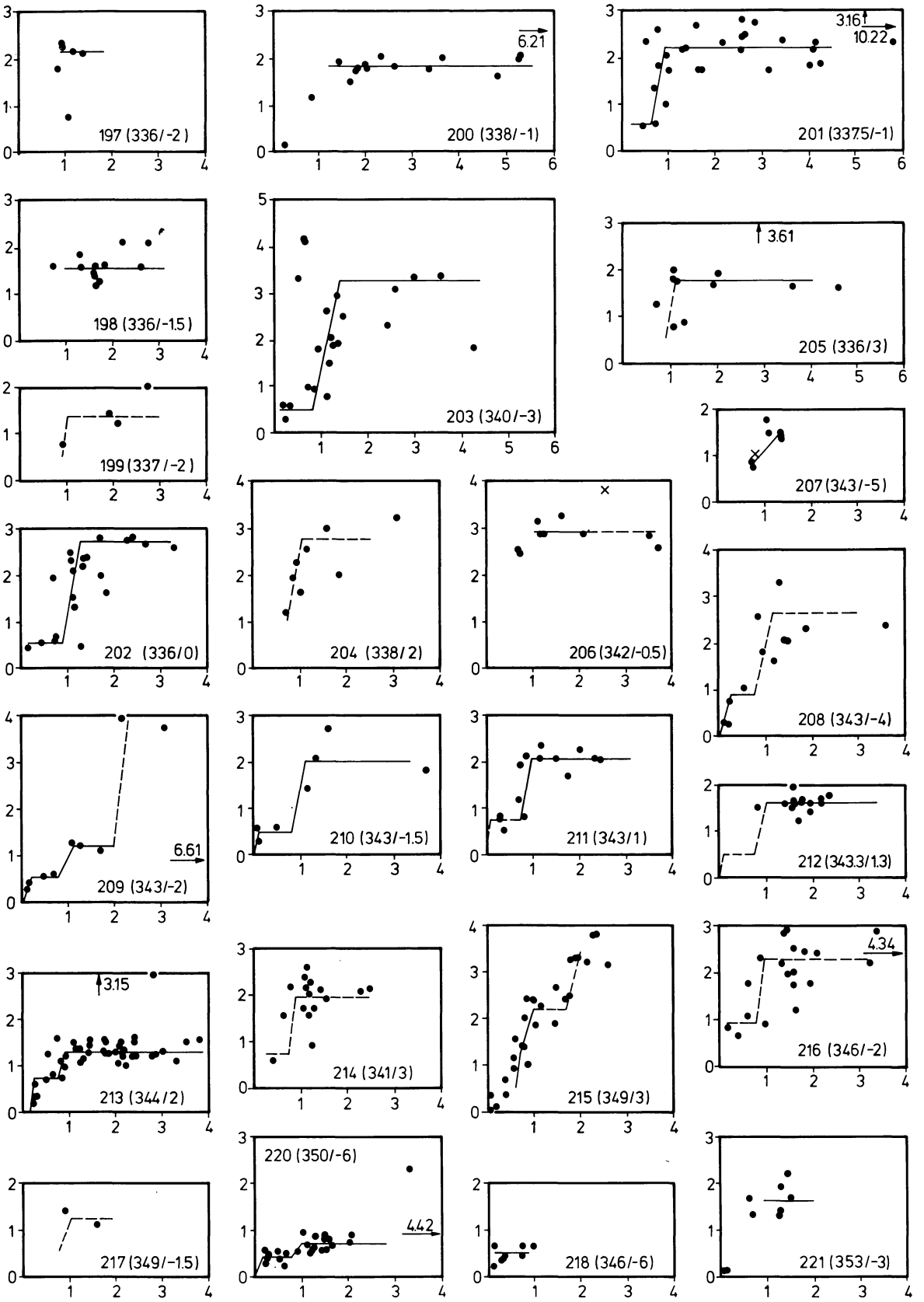

FIGURE 6j.

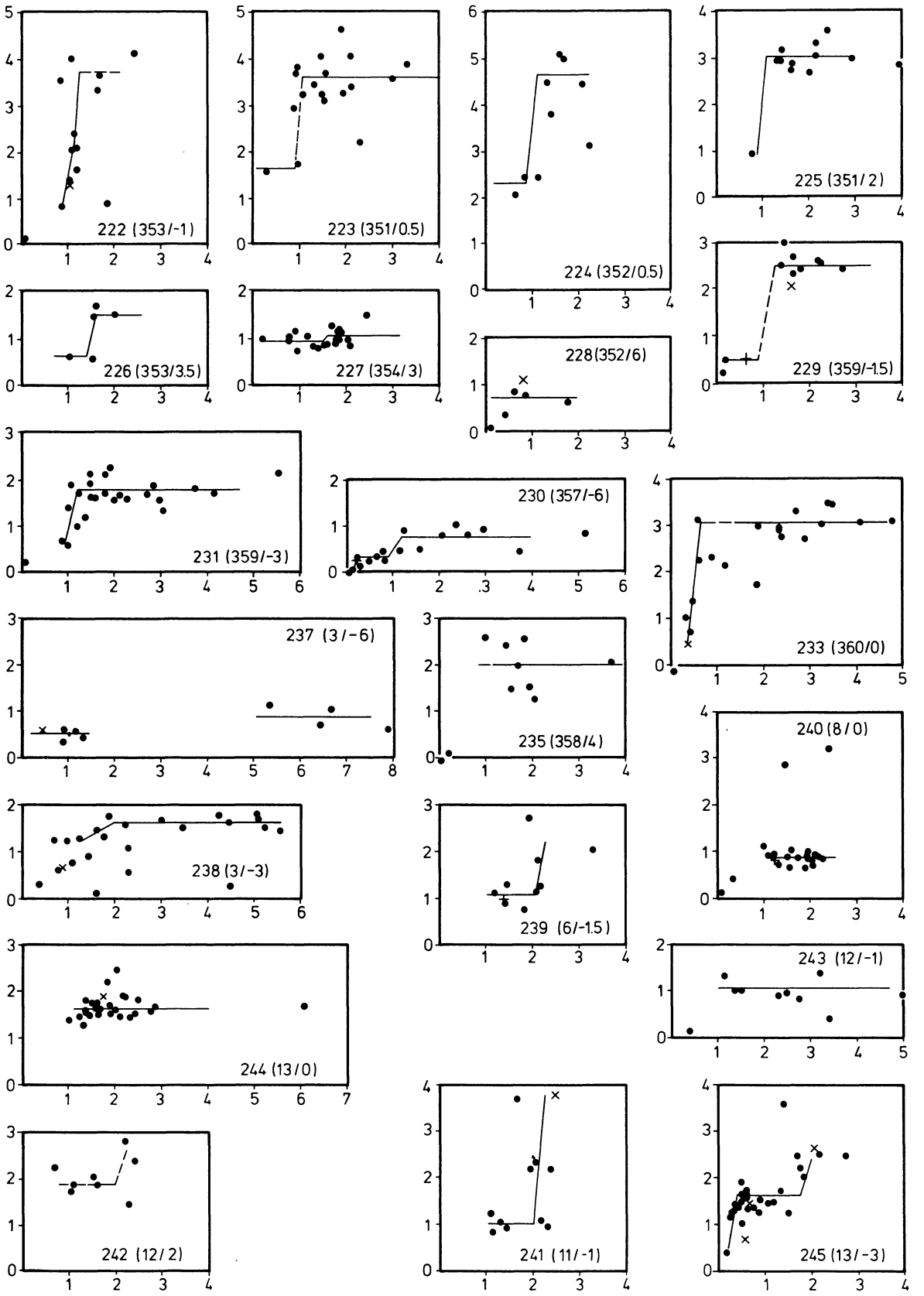

FIGURE 6k.

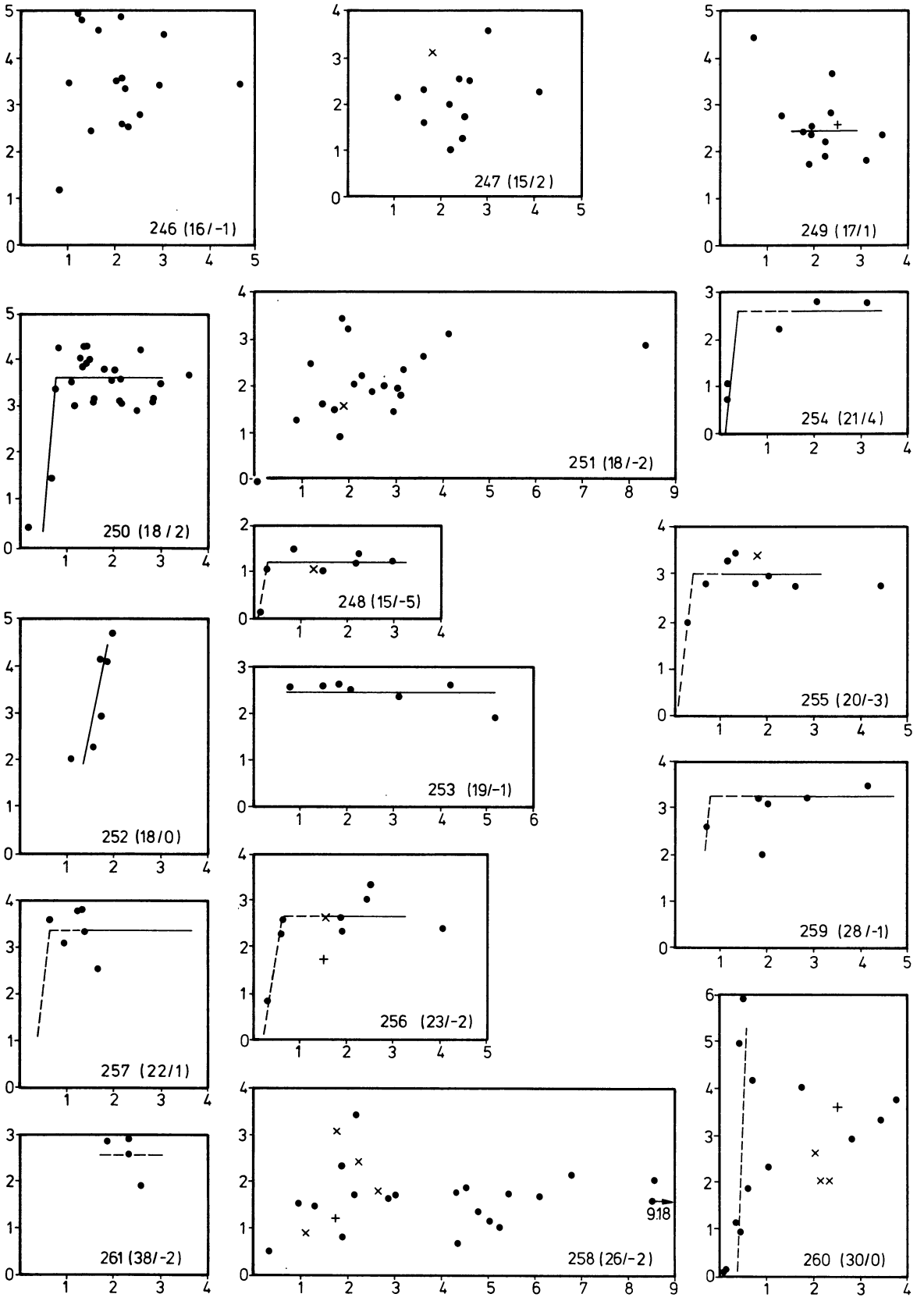

FIGURE 61.

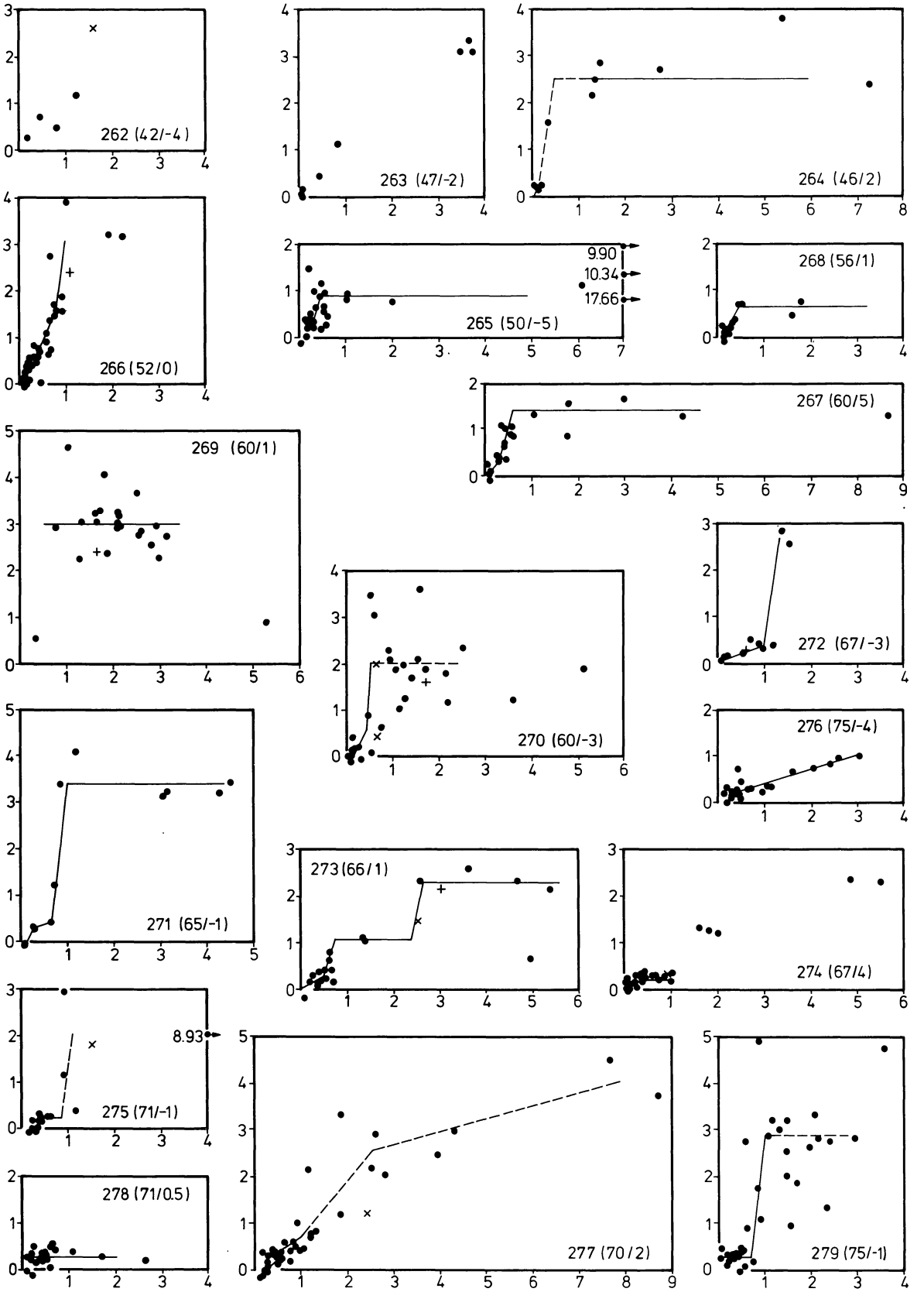

FIGURE 6m.

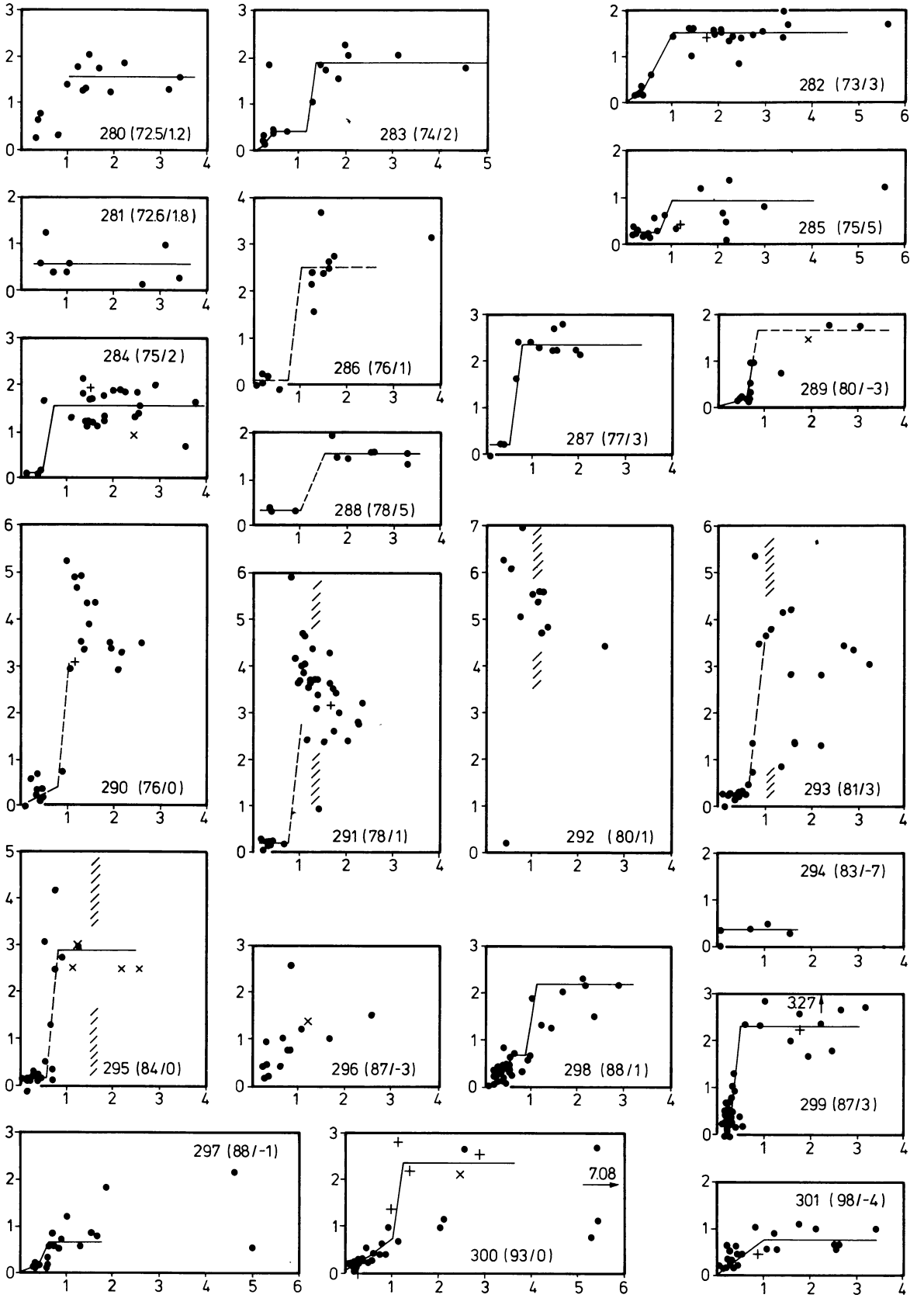

FIGURE 6n.

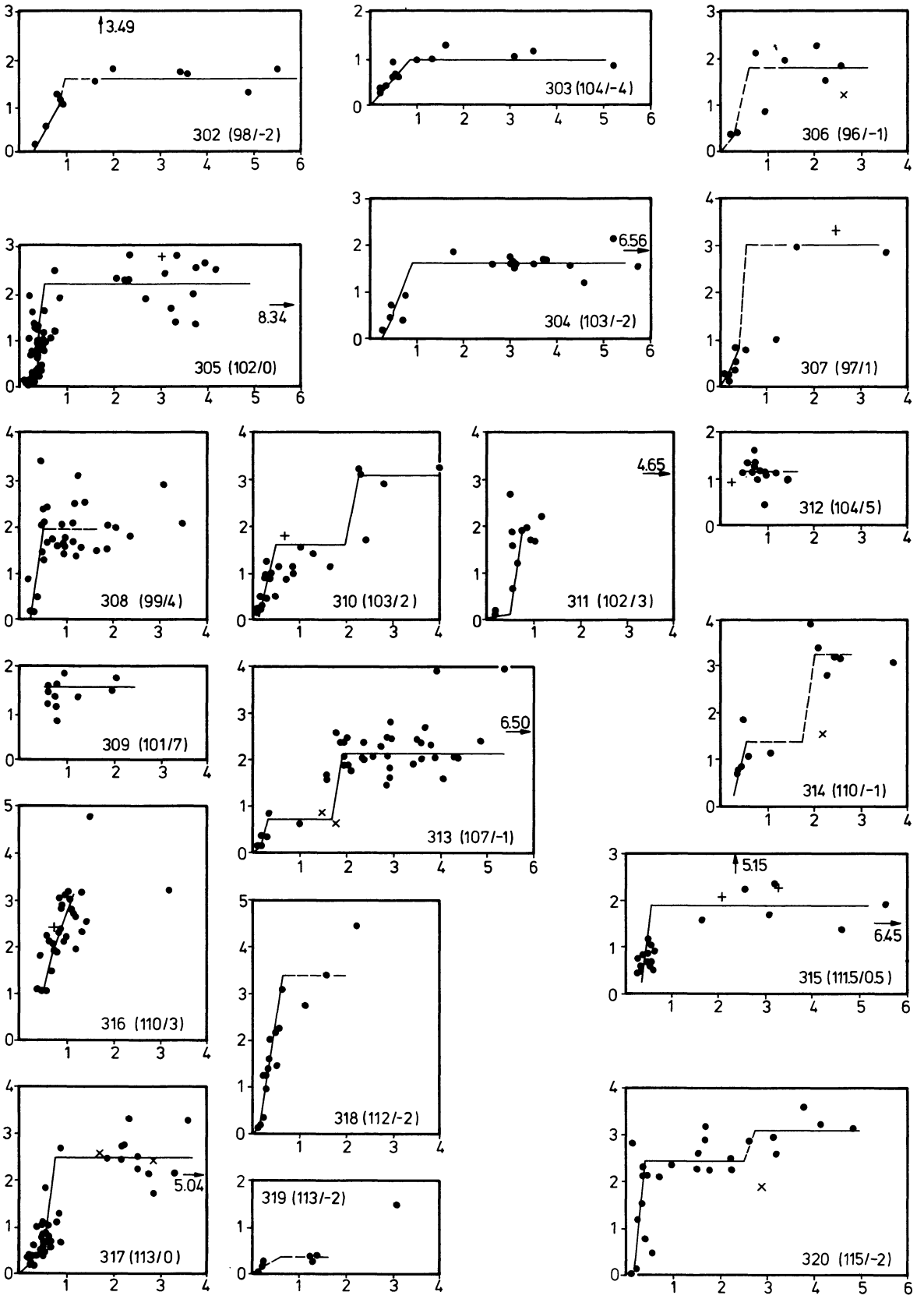

FIGURE 6o.

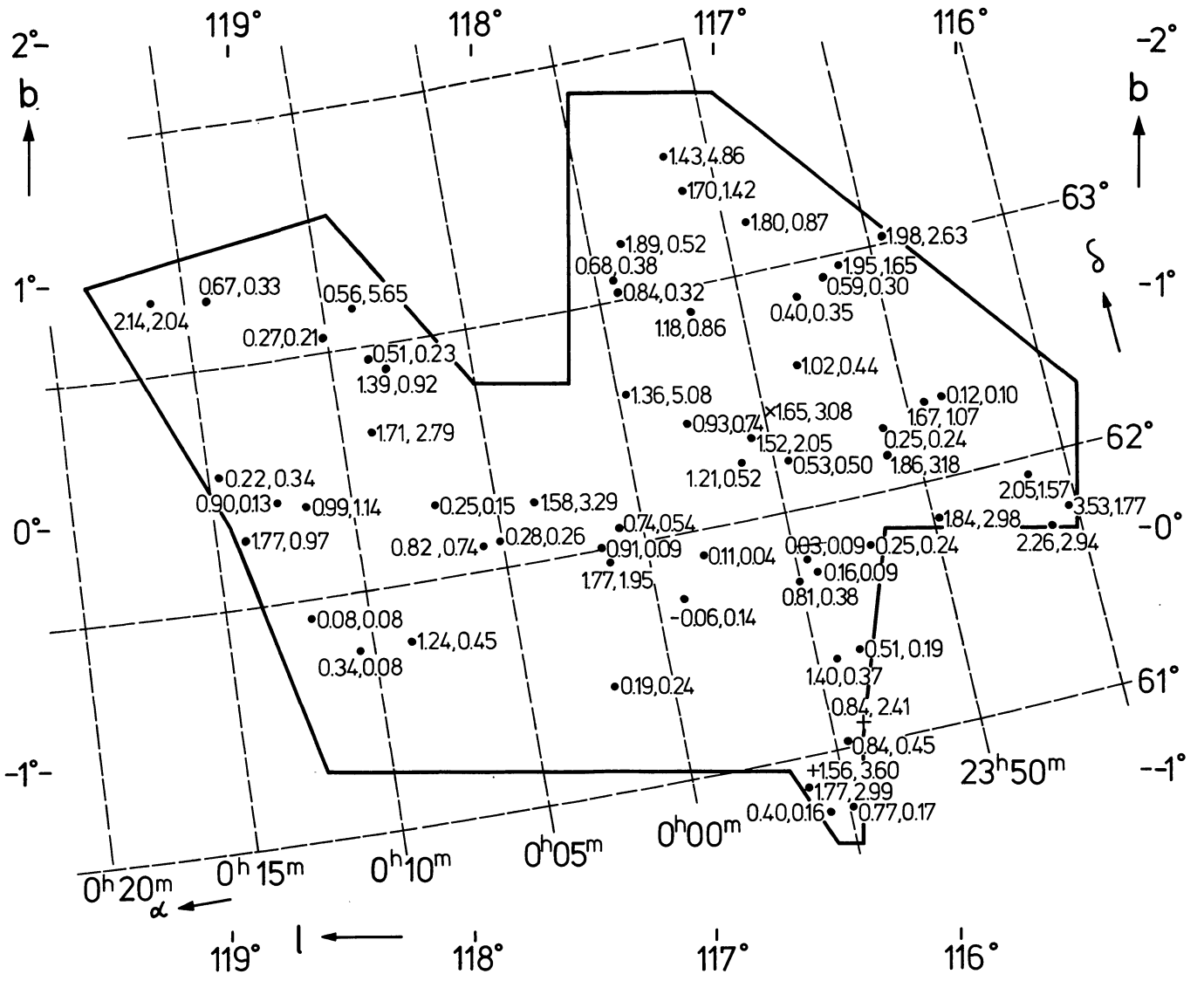

FIGURE 7. — Map of field 1. Dots denote O-F stars, upright crosses galactic clusters and diagonal crosses δ Cephei stars. The numbers give the extinction A_v in magnitudes and the distance in kpc.

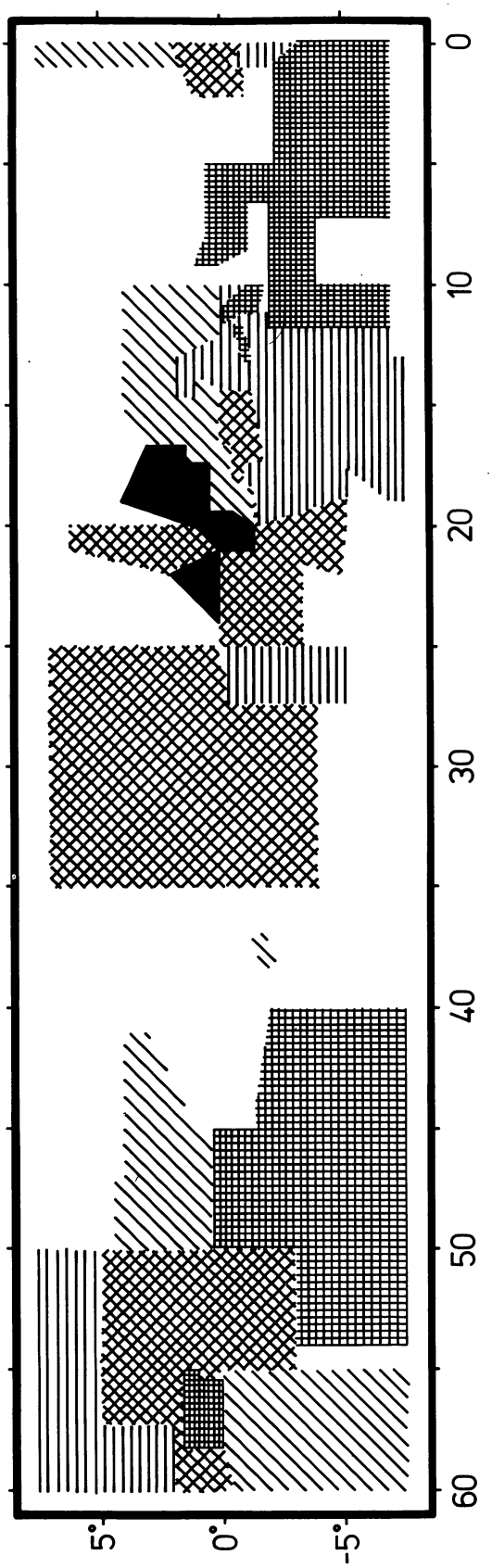

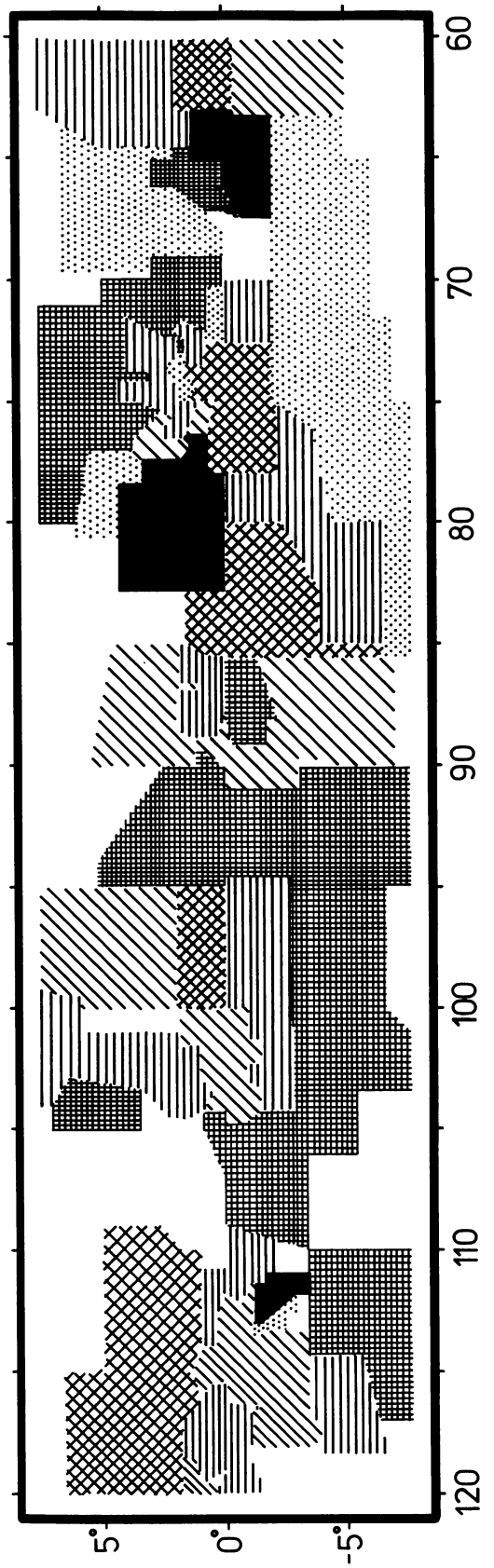

FIGURE 8a.

FIGURE 8. — The extinction at $r = 1$ kpc in the Milky Way.
$A_v < 0^m.5$ $1^m.9 \leq A_v < 2^m.6$
$0.5 \leq A_v < 1.2$ $2^m.6 \leq A_v < 3^m.3$
$1^m.2 \leq A_v < 1^m.9$ $A_v \geq 3^m.3$

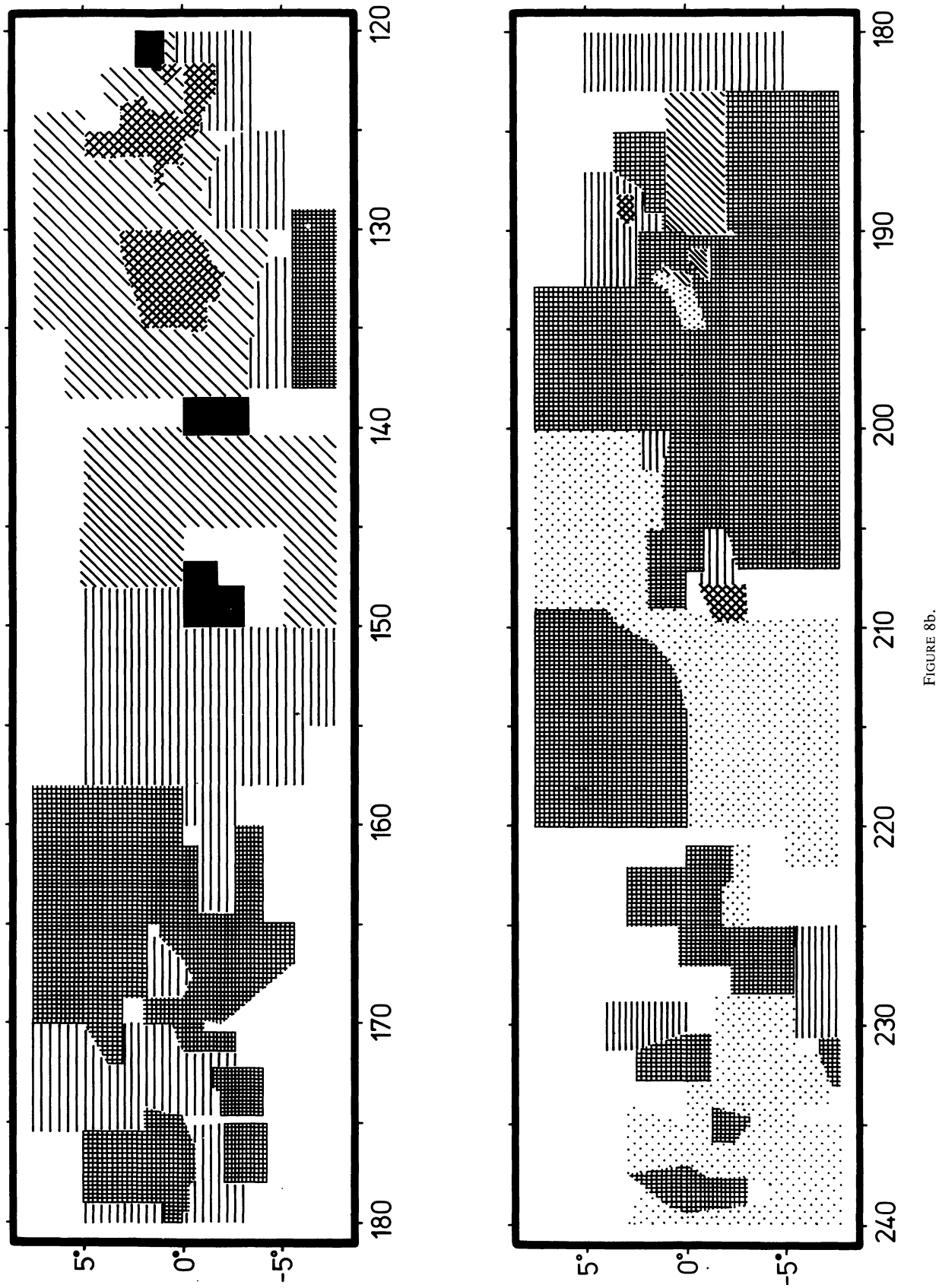

FIGURE 8b.

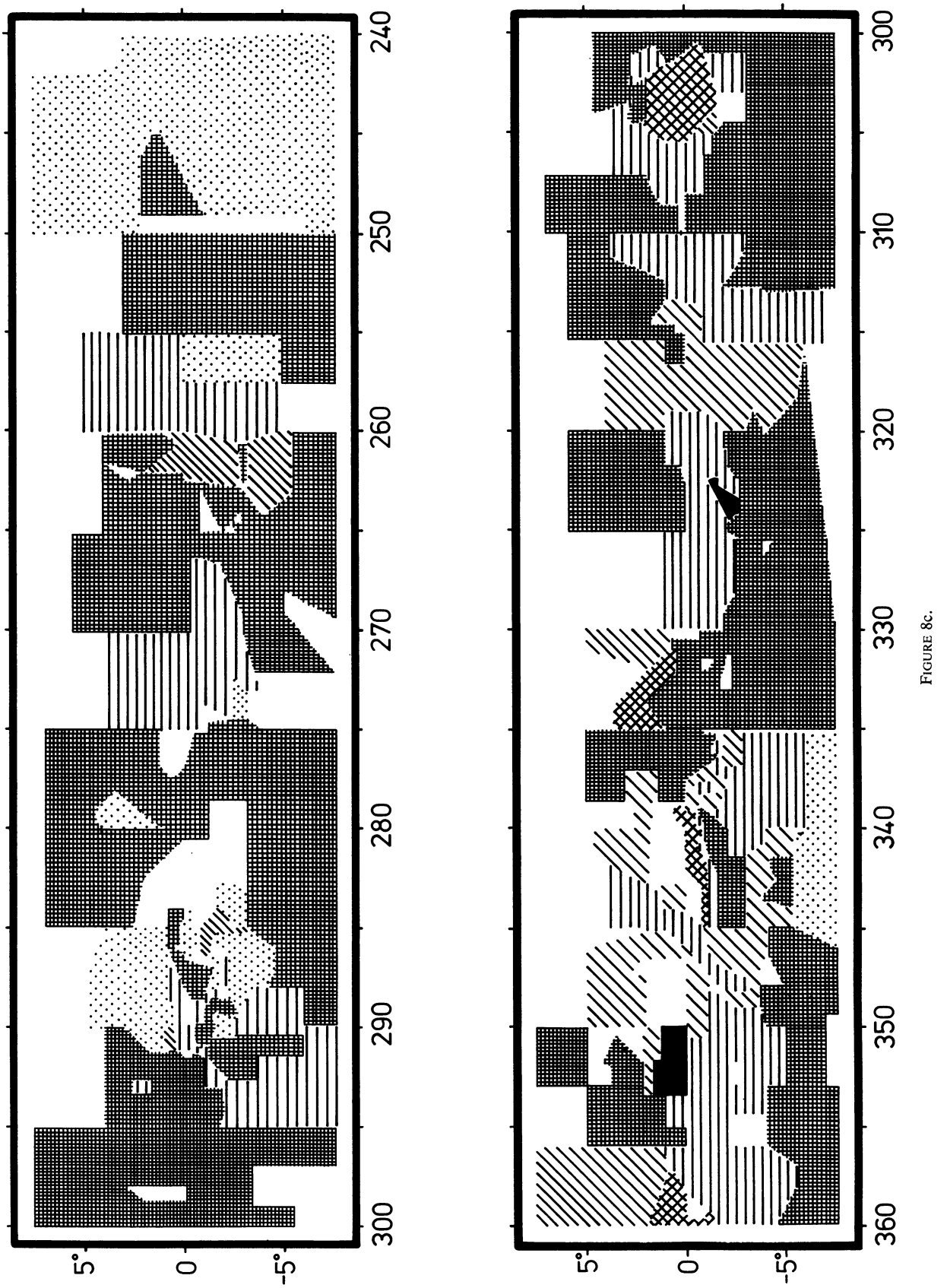

FIGURE 8c.

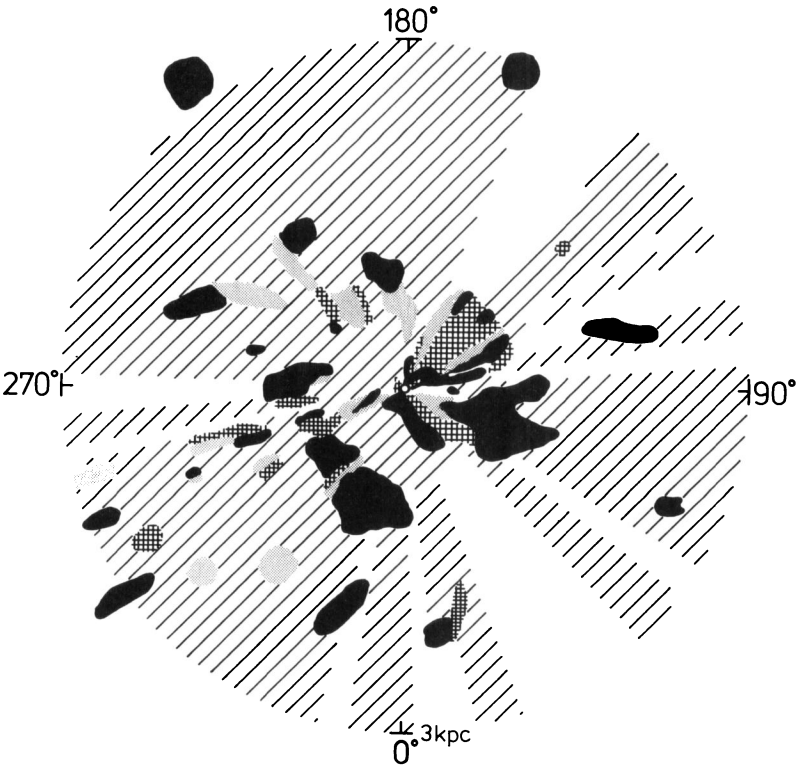

FIGURE 9a. — The galactic distribution of the dust for $r \leq 3$ kpc

$a_v = A_v/\text{kpc} < 1^m0/\text{kpc}$
$1^m0/\text{kpc} \leq a_v < 2^m0/\text{kpc}$
$2^m0/\text{kpc} \leq a_v < 3^m0/\text{kpc}$
$a_v \geq 3^m0/\text{kpc}$

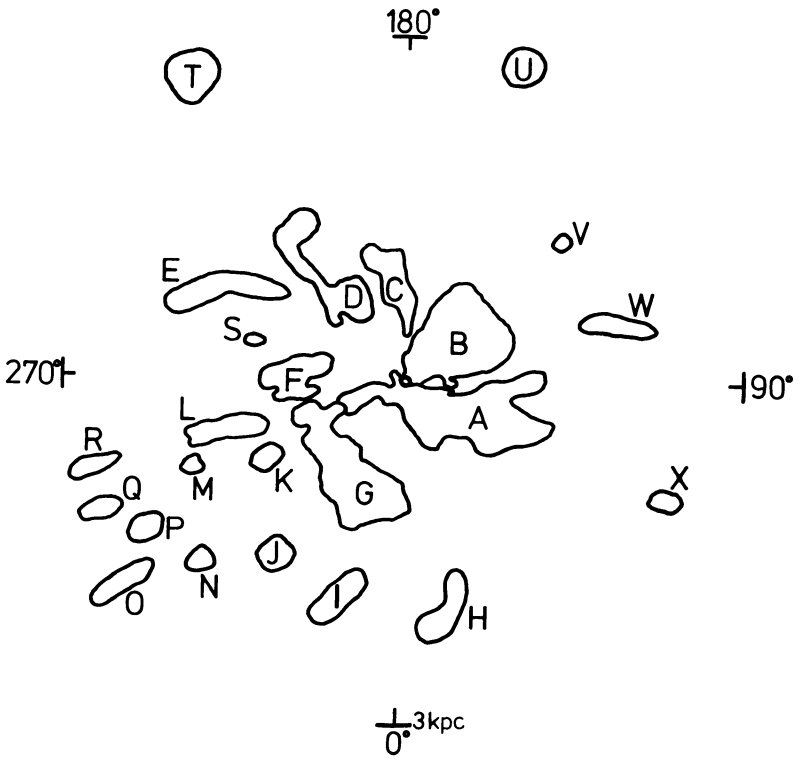

FIGURE 9b. — Notation of the dust clouds outlined in figure 9a.